Small Signal Stability Improvement of a Single Machine Infinite Bus System Using a Static VAR Compensator

DISSERTATION
SUBMITTED IN PARTIAL FULFILLMENT OF THE REQUIREMENTS
FOR THE AWARD OF THE DEGREE
OF

MASTER OF TECHNOLOGY
IN
Electrical Engineering (Power Systems)

Submitted by:

Raju Meena

(2K13/ PSY/ 14)

Under the supervision of

Dr.SumanBhowmick

DEPARTMENT OF ELECTRICAL ENGINEERING

DELHI TECHNOLOGICAL UNIVERSITY

(Formerly Delhi College of Engineering)

Bawana Road, Delhi-110042

2015

CERTIFICATE

I, **RajuMeena**, Roll No. 2K13/PSY/14 student of M. Tech. (Power System), hereby declare that the dissertation titled "**Small Signal Stability Improvement of a SMIB System Using a Static Var Compensator**" under the supervision of **Dr.Suman Bhowmick**, Electrical Engineering Department, Delhi Technological University, in partial fulfilment of the requirement for the award of the degree of Master of Technology, has not been submitted elsewhere for the award of any degree.

Place: Delhi **(Raju Meena)**

Date:

(Dr.Suman Bhowmick)

Associate Professor

Department of Electrical Engineering

Delhi Technological University

Bawana Road, Delhi-110042

ACKNOWLEDGEMENT

First and foremost, I express my sense of gratitude to my supervisor Dr. Suman Bhowmick, Associate Professor, Department of Electrical Engineering, Delhi Technological University for his guidance, supervision, support, motivation and encouragement throughout the period this work was carried out. His readiness forconsultation at all times, his educative comments, his concern and assistance has been invaluable.

I wish to take this opportunity to express my gratitude to Prof. Madhusudan Singh, Head of the department of Electrical Engineering for his constant encouragement during the conduct of the project work. I express my gratitude to all the faculty members of Electrical Department for their motivations from time to time.

I also thank all the non-teaching staff of the Electrical Engineering Department for their fullest cooperation.

I would like to thank all those who have directly or indirectly helped me in completion of the thesis well in time.

Finally, I wish to thanks my parents for their moral support and confidence showed in me to pursue M.Tech at an advanced stage of my academic career.

Delhi, 2015 RajuMeena

ABSTRACT

The small signal stability of a power system is the ability of the system to maintain synchronism under small disturbances like variation in load and/or generation. The disturbances are considered sufficiently small for linearization of system equations to be permissible for the purpose of analysis. Traditional ways to improve small signal stability included power system stabilizers (PSS). Shunt FACTS Controllers like Static Var Compensator (SVC) are primarily used to improve the voltage profile and for reactive power compensation. SVC susceptance modulation using a damping controller can achieve the additional objective of power oscillation damping. It is observed that SVC with only voltage controller increases the small signal stability marginally. However, when a damping controller is added, a marked increase in the system small signal stability is observed. A damping controller can use a variety of auxiliary or supplementary signals to improve the power oscillation damping. Usually, at the SVC location, electrical power, synthesized frequency, line current etc. are used as auxiliary signals. In this work, line current signal is used as a supplementary signal, with the SVC connected at the mid-point of the transmission line. Multiple case studies with a SMIB system validate this.

CONTENTS

LIST OF FIGURES

LIST OF SYMBOLS

SSS	Small Signal Stability
SMIB	Single Machine Infinite Bus
SVC	Static Var Compensator
$\Delta\omega_r$	Per unit speed deviation
δ	Rotor angle (elec rad.)
$\Delta\delta$	Rotor angle deviation (elec. rad.)
ω_0	Base rotor angular speed (elec. rad/sec)
p	Differential operator d/dt
s	Laplace operator
K_S	Synchronizing torque coefficient
K_D	Damping torque coefficient
E'	Generator voltage behind transient reactance
E_B	Infinite bus voltage
E_t	Generator terminal voltage
X_E	Equivalent reactance
X_{line}	Transmission line reactance
X_t	Transformer reactance
X_{svc}	SVC reactance
B_{svc}	SVC susceptance
T_e	Air gap torque
Ψ_{fd}	Field circuit dynamics
α	SVC firing angle
E_{fd}	Exciter output voltage
ξ	Damping ratio
λ	Eigenvalue
H	Inertia constant
A	System state matrix
B	Control input matrix
C	Output matrix
X	Vector of state variables

Y Output vector

K Control gain

u Control input vector

I_{svc} SVC current

I_t Generator current

I_{line} Transmission line current

V_m Transmission line midpoint voltage

e_d d-axis component of generator terminal voltage

e_q q-axis component of generator terminal voltage

I_d d-axis component of generator terminal current

I_q q-axis component of generator terminal current

I_{fd} Field current

ψ_d, ψ_q Stator and Rotor flux linkages

ψ_{ad}, ψ_{aq} Mutual flux linkages

L_{ads}, L_{aqs} Mutual inductance

K_{sd}, K_{sq} Total saturation factor

CHAPTER 1

INTRODUCTION

1.1 BASIC CONCEPT AND DEFINITIONS

Power system stability may be broadly defined as that property of a power system that enables it to remain in a state of operating equilibrium under normal operating conditions and to regain an acceptable state of equilibrium after being subjected to a disturbance.

Small signal stability is the ability of the power system to maintain synchronism under small disturbances. Such disturbances occur continually on the system because of small variation in load and generation. The disturbances are considered sufficiently small for linearization of system equations to be permissible for the purpose of analysis. Instability that may result can be of two forms:

(1) Steady increase in rotor angle due to lack of sufficient synchronizing torque or

(2) Rotor oscillations of increasing amplitude due to lack of sufficient damping torque.

The nature of system response to small disturbances depends on a number of factors including the initial operating condition, the transmission system strength, and the type of generator excitation controls used.

In today's practical power system, small signal stability is largely a problem of insufficient damping of oscillations.

Traditional ways to improve small signal stability included power system stabilisers (PSS).

FACTS Controllers like Static Var Compensator (SVC) can be used to improve power transfer capability by improving system bus voltage profile.

In this work, the small signal stability of a single machine infinite bus (SMIB) system is analysed. In this system, the generator is connected to the infinite bus through a step up transformer and a long transmission line. The SVC is connected at the mid-point of the transmission line.

It is observed that SVC with only voltage controller marginally increases the system small signal stability. However, when a damping controller is added, a marked increase in the system small signal stability is observed.

A damping controller can use a variety of auxiliary or supplementary signals to improve the power oscillation damping. Usually, deviations in the rotor speed, electrical power, line current etc. are used as auxiliary signals. In this work, line current is used as the auxiliary signal.

1.2 LITERATURE REVIEW

Power system stability is a topic that has always challenged power system engineers. A review of the history of the subject is useful for a better understanding of present day stability problems.

The stability of power systems was first recognized as an important problem in 1920. Results of the first laboratory tests on miniature systems were reported in 1924. The first field test on the stability on a practical power system was conducted in 1925.

[1] presents terms and definitions in the analysis of Power System Stability. This paper also gives the mathematical analysis of representing the d-axis and q-axis saturation in the small perturbation of a synchronous machine. The analysis is performed for a synchronous machine connected to an infinite bus system through a transmission line.

[2] describes the modelling techniques for the small signal stability analysis of a single machine infinite bus system by Phillips-Heffron model and the eigenvalue analysis. It also presents the use of the participation factors for identifying the relevant swing modes.

[3] presents the small signal stability of nonlinear system as given by the roots of characteristic equation of the system i.e., by the eigenvalues of state matrix A.

[4] describes participation factor for analysing a system.

[5] describes the eigenvalue computation by solving the characteristic equation of a simple second-order system. Using the state space representation and modal analysis, the torque-angle relationship is used to analyze the system stability characteristics.

The block diagram approach was first used by Heffron and Phillips[6] and later by deMello and Concordia[7] to analyze the small signal stability of a synchronous machine connected to a power system.

CIGRE defines a static var system (SVS) as a combination of a static var compensator (SVC) and mechanically switched capacitors and reactors, all under coordinated control [8]. Most of this paper pertains to the modeling of static var compensators.

Speed deviation is used as the supplementary control signal as described in [9]. However, at the mid-point of the line, the speed deviation signal may not be available. Hence, other supplementary signals like line current, frequency deviation, deviation of line active power etc. may be used.

[10] describes static var compensator models for power flow and dynamic analysis.

The influence of dynamic devices on the behavior of different electromechanical modes can be explained through the associated synchronizing and damping torques by modal analysis as in [11], [12].

The Philips Heffron block diagram model of a single machine infinite bus system installed with an SVC, incorporating a damping controller using a supplementary input signal is described in [11,13,14].

Power system damping enhancement by application of SVC has been described in [15] based on the well-known equal area criterion.

Use of dynamic reactive power compensation to improve voltage and reactive power conditions in a SMIB system is described in [16]. It is shown that additional tasks can also be performed by an static Var Compensator (SVC) to increase the transmission capacity when a SVC is used for power oscillation damping.

[17] has reported that damping control introduced by the SVC ia able to provide the power system with damping whose capability increases at higher level of load.

[18] describes the application of Static Var Systems for enhancing system dynamic performance.

[19] presents the results of a recent EPRI-sponsored study to compare the performance of GTO-based systems with conventional SVCs and synchronous condensers, so that decisions for development and eventual procurement of such systems can be made on a rational technical and economic basis.

[20-21] presents the various measurement systems employed in the SVC control system. The demodulation effect of the measurement systems was discussed in detail. The different components of the basic SVC voltage control system are described.

[22-25] presented different control issues related to the voltage-control function of the SVC. The procedures for design of voltage regulator are described, and the influences of network resonances and harmonic resonances on the performance of SVC voltage control are also discussed.

The advantage achieved by adopting the voltage-modulation control strategy, in comparison to constant-voltage regulation, is presented in ref. [26].

The optimal robust control and H_∞ optimization are described in [27, 28]

SVC with a primary-voltage control loop and an auxiliary controller with generator-speed deviation as the control signal [29].

An SVC with a single-input–signal-output (SISO) proportional–integral derivative (PID) auxiliary-speed controller, in conjunction with a voltage regulator, is proposed in [30] for damping torsional oscillations.

An concept is described in [31], in which a midline-located SVC in a series-compensated SMIB system is used for power-transfer improvement.

[32] presents a fundamental analysis of the application of static VAr compensators (SVC) for stabilizing power systems. Basic SVC control strategies are examined in terms of enhancing the dynamic and transient stabilities, improving tie line transmission capacity and damping power oscillations.

1.3 ORGANISATION OF THE THESIS

In this thesis, the small signal stability of a single machine infinite bus (SMIB) system incorporated with a Static Var Compensator (SVC) at the midpoint of transmission line, is analysed. The SVC is equipped with a voltage controller and a damping controller which uses line current magnitude as the auxiliary signal. The thesis consists of five chapters.

Chapter one presents an overview of the general ideas about stability, the SVC as a shunt connected FACTS controller and related works.

Chapter two describes the small signal stability model of single machine infinite bus system.

Chapter three describes the SVC Voltage controller and damping controllers.

Chapter four addresses the modelling of a single machine infinite bus system with SVC voltage and damping controller.

Chapter five presents the different case studies taken up for analysis and the results.

.

CHAPTER-2

SMALL SIGNAL STABILITY OF A SINGLE MACHINE INFINITE BUS SYSTEM

2.1 INTRODUCTION

Small signal stability is the ability of the system to maintain synchronism under small disturbances like change in loads or generation. Such disturbances occur continually on the system because of small variation in load and generation. The disturbances are considered sufficiently small for linearization of system equations to be permissible for the purpose of analysis. Traditional ways to improve small signal stability included power system stabilisers (PSS). The general system configuration for a single machine infinite bus system is shown in fig 2.1(a). For the purpose of analysis, the system of fig 2.1(a) can be reduced to the form of fig 2.1(b) by using Thevenin's equivalent of the transmission network external to the machine and the adjacent transmission system.

We will analyze the small signal stability of the system of Fig 2.1(b) with the synchronous machine represented by models of varying degrees of detail. We will begin with the classical model and gradually increase the model detail by accounting for the effects of the dynamics of the field circuit, and the excitation system.

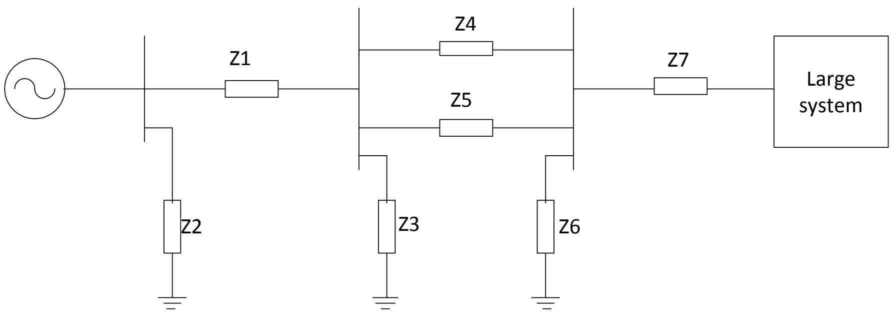

Fig 2.1(a): A single machine connected to a large power system through transmission lines

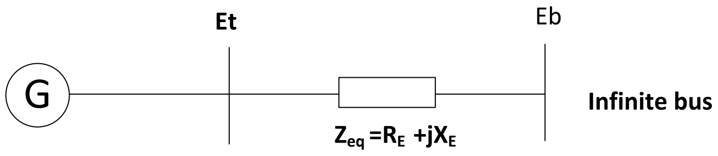

Fig 2.1(b): Equivalent circuit of the system shown in Fig. 2.1 (a)

2.2 GENERATOR REPRESENTED BY THE CLASSICAL MODEL

The system representation is shown in Fig 2.2.The generator is represented the classical model and all resistances neglected. Here E' is the voltage behind Xd'. Its magnitude is assumed to remain constant at the pre-disturbance value. Let δ be the angle by which E' leads the infinite bus voltage Eb. As the rotor oscillates during a disturbance, δ changes.

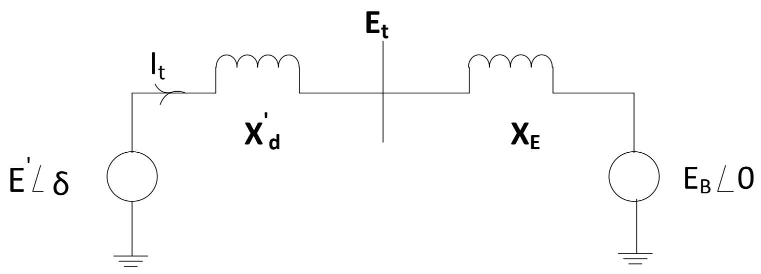

Fig 2.2 SMIB system with generator represented by the classical model

From Fig 2.2, with E' as the reference phasor, the generator current is given by

$$\tilde{\mathbf{I}}_{\mathbf{t}} = \frac{E'\angle 0 - E_B\angle -\delta}{jX_T}$$

$$\tilde{\mathbf{I}}_{\mathbf{t}} = \frac{\mathrm{E}' - \mathrm{E_B}\,(\cos\delta - \mathrm{j}\sin\delta)}{\mathrm{jX_T}} \qquad (2.1)$$

$$\tilde{\mathbf{E}}' = \tilde{\mathbf{E}}_{\mathbf{t0}} + \mathbf{j}\mathrm{X'_d}\tilde{\mathbf{I}}_{\mathbf{t0}}$$

$$X_T = X'_d + X_E$$

The complex power behind X'_d is given by

$$\boldsymbol{S}' = P + jQ'$$

$$= \frac{E' E_B \sin\delta}{X_T} + \frac{E'(E' - E_B \cos\delta)}{X_T} \tag{2.2}$$

With armature resistance neglected, the air gap power is equal to the terminal power ‘P’. In p.u., the air-gap torque is equal to the air-gap power,

Hence,

$$T_e = P = \frac{E' E_B}{X_T} \sin\delta \tag{2.3}$$

We linearize the expression for the air-gap torque around the operating point.

Linearizing about an operating condition represented by $\delta = \delta_0$.

$$\Delta T_e = \frac{\partial T_e}{\partial \delta} \Delta\delta \tag{2.4}$$

$$= \frac{E' E_B}{X_T} \cos\delta_0 (\Delta\delta)$$

Basic equation of motion :-

The basic electromechanical equation, also known as the swing equation, is given by

$$\frac{2H}{\omega_0} p^2 \delta = (T_m - T_e - K_D \Delta\omega_r)$$

It can be observed that the swing equation is a 2nd order nonlinear differential equation and can be represented by two first order differential equations. These are

$$p\Delta\omega_r = \frac{1}{2H} (T_m - T_e - K_D \Delta\omega_r) \tag{2.5}$$

$$p\delta = \omega_0 \Delta\omega_r \tag{2.6}$$

where

$\Delta\omega_r$ = per unit speed deviation

δ = rotor angle (elec rad.)

ω_0 = Base rotor electrical speed (rad/sec)

p = Differential operator d/dt (time in sec)

Linearizing equation (2.5) and putting the value of ΔT_e from equation (2.4), we get,

$$p\Delta\omega_r = \frac{1}{2H}(\Delta T_m - K_S\Delta\delta - K_D\Delta\omega_r) \qquad (2.7)$$

where ΔT_m is considered as change in mechanical torque and

$$K_S = \frac{E' E_B}{X_T}\cos\delta_0 \qquad (2.8)$$

In the above equation, K_S is the synchronizing torque coefficient

Linearizing equation (2.6), we get

$$p\Delta\delta = \omega_0\Delta\omega_r \qquad (2.9)$$

Writing Equations (2.7) and (2.9) in the vector matrix form, we obtain

$$\frac{d}{dt}\begin{bmatrix}\Delta\omega_r \\ \Delta\delta\end{bmatrix} = \begin{bmatrix}-\frac{K_D}{2H} & -\frac{K_S}{2H} \\ \omega_0 & 0\end{bmatrix}\begin{bmatrix}\Delta\omega_r \\ \Delta\delta\end{bmatrix} + \begin{bmatrix}\frac{1}{2H} \\ 0\end{bmatrix}\Delta T_m \qquad (2.10)$$

Equation (2.10) is in this form $\dot{\mathbf{x}} = \mathbf{Ax} + \mathbf{Bu}$. The element of the state matrix **A** are dependent on the parameters K_D, H, X_T and the initial operating values of E' and δ_0.

Taking the Laplace transformation of equations (2.7) and (2.9), we get,

$$s\Delta\omega_r(s) = \frac{1}{2H}\left(\Delta T_m(s) - K_S\Delta\delta(s) - K_D\Delta\omega_r(s)\right)$$

$$\Delta\omega_r(s) = \frac{1}{2Hs}\{\Delta T_m(s) - K_S\Delta\delta(s) - K_D\Delta\omega_r(s)\} \qquad (2.11)$$

$$s\Delta\delta(s) = \omega_0\Delta\omega_r(s)$$

$$\Delta\delta(s) = \frac{\omega_0}{s}\Delta\omega_r(s) \tag{2.12}$$

These equations are represented in the transfer function block diagram as shown in Fig. 2.3.

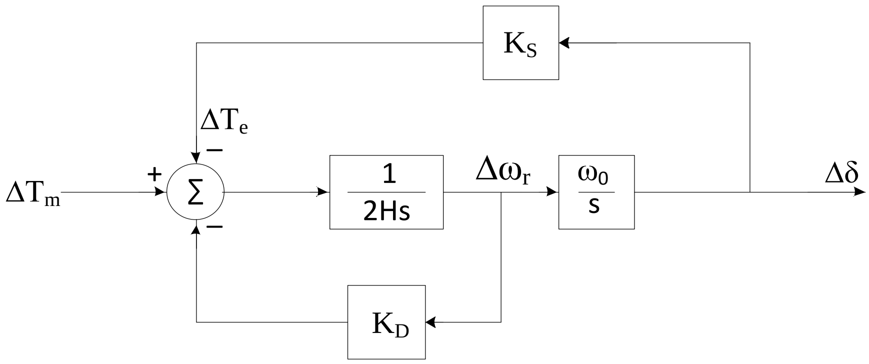

Fig 2.3: Transfer function block diagram of SMIB system

Simplifying equations (2.11) and (2.12), we get,

$$\Delta\delta = \frac{\omega_0}{s}\left[\frac{1}{2Hs}\{\Delta T_m - K_S\Delta\delta - K_D\Delta\omega_r\}\right]$$

$$\Delta\delta = \frac{\omega_0}{s}\left[\frac{1}{2Hs}\left\{\Delta T_m - K_S\Delta\delta - K_D s\frac{\Delta\delta}{\omega_0}\right\}\right] \tag{2.13}$$

Rearranging,

$$s^2(\Delta\delta) + \frac{K_D}{2H}s(\Delta\delta) + \frac{K_s}{2H}\omega_0(\Delta\delta) = \frac{\omega_0}{2H}\Delta T_m$$

Therefore, the characteristic equation is given by

$$s^2 + \frac{K_D}{2H}s + \frac{K_s}{2H}\omega_0 = 0 \tag{2.14}$$

The characteristic equation is in the general form of

$$s^2 + 2\xi\omega_n s + {\omega^2}_n = 0$$

Roots of this equation are

$$s = -\xi\omega_n \pm j\omega_n\sqrt{1-\xi^2}$$

$$= \sigma \pm j\omega$$

The real part of the eigenvalues gives the damping and the imaginary part of the eigenvalues gives the frequency of the oscillation. A negative real part indicates a damped oscillation whereas a positive real part indicates oscillation of increasing amplitude.

The pair of eigenvalues are

$$\lambda = \sigma \pm j\omega$$

The frequency of damped oscillation is in Hz is given by

$$f = \frac{\omega}{2\Pi}$$

The damping ratio is given by

$$\xi = \frac{-\sigma}{\sqrt{\sigma^2 + \omega^2}}$$

The damping ratio 'ξ' determines the rate of decay of the amplitude of the oscillation.

When $0 \le \xi \le 1$, the system is under damped

$\xi = 1$ critically damped

$\xi > 1$ over damped

If $\xi < 0$, the system is unstable

In any system, we have to ensure that the damping is adequate so that the oscillations generated in the system are damped. Whenever we design the controller for the system we have to achieve a minimum damping for all the modes which are present in the system.

Thus, from equation (14), the undamped natural frequency is

$$\omega_n = \sqrt{K_s \frac{\omega_0}{2H}} \text{ rad/s} \qquad (2.15)$$

and the damping ratio is

$$\xi = \frac{1}{2}\frac{K_D}{2H\omega_n} = \frac{1}{2}\frac{K_D}{\sqrt{K_s 2H\omega_0}} \quad (2.16)$$

From equations (2.15) and (2.16), it can be observed that when the synchronizing torque coefficient K_s increases, then ω_n increases and ξ decreases. An increase in damping torque coefficient K_D increases ξ whereas an increase in inertia constant decreases both ω_n and ξ.

2.3 EFFECTS OF SYNCHRONOUS MACHINE FIELD CIRCUIT DYNAMICS :

We now consider the system performance including the effect of field flux variations. The amortisseur effect will be neglected and the field voltage will be assumed constant (manual excitation control).

A state-space model of the system is developed by first reducing the synchronous machine equations to an appropriate form and then combining them with network equations. We will express time in seconds, angles in electrical radians, and all other variables in per unit.

2.3.1 Synchronous machine equations

As in the classical generator model, the acceleration equations are

$$p\Delta\omega_r = \frac{1}{2H}(T_m - T_e - K_D\Delta\omega_r) \quad (2.17)$$

$$p\delta = \omega_0\Delta\omega_r \quad (2.18)$$

where

$$\omega_0 = 2\Pi f_0 \text{ elec. rad/s.}$$

In this case, the angle by which the q-axis leads by reference E_B is the rotor angle δ. As shown in the Fig (2.4), the rotor angle δ is the sum of the angle δ_i (internal angle) and the angle of Et leads E_B. For identifying the rotor position with respect to an appropriate reference and keeping track of it as the rotor oscillates, the q-axis is used. The choice of E_B as the reference for measuring rotor angle is convenient from the viewpoint of solution of network equations.

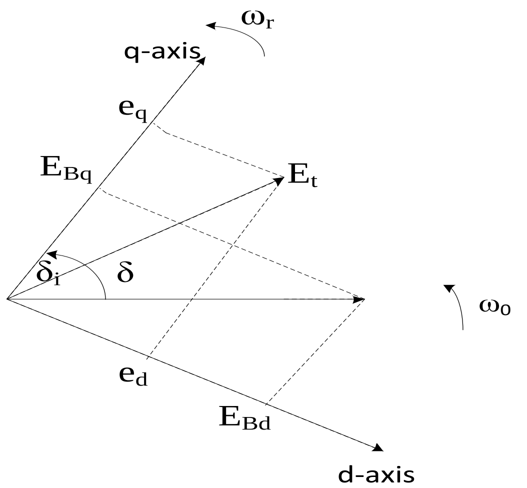

Fig 2.4 Relation between d-axis and q-axis quantities

The field circuit dynamic equations is

$$p\Psi_{fd} = \omega_0(e_{fd}+R_{fd}i_{fd})$$

$$= \frac{\omega_0 R_{fd}}{L_{adu}} E_{fd} - \omega_0 R_{fd} i_{fd} \quad (2.19)$$

where $e_{fd} = \frac{R_{fd}}{L_{adu}} E_{fd}$

where E_{fd} is the exciter output voltage. Equations (2.17) – (2.19) describe the dynamics of the synchronous machine with $\Delta\omega_r$, δ and $\Psi\psi_{fd}$ are the state variables.

The Rotor and Stator flux linkages are given by

$$\Psi_d = -L_1 i_d + L_{ads}(-i_d + i_{fd})$$

$$= -L_1 i_d + \Psi_{ad} \quad (2.20)$$

$$\Psi_q = -L_1 i_q + L_{aqs}(-i_q)$$

$$= -L_1 i_q + \Psi_{aq} \quad (2.21)$$

$$\Psi_{fd} = L_{ads}(-i_d + i_{fd}) + L_{fd} i_{fd}$$

$$= \Psi_{fd} + L_{fd} i_{fd} \tag{2.22}$$

where

Ψ_{ad} , Ψ_{aq} =Air-gap (mutual) flux linkages

L_{aqs} = Saturated values of the mutual inductances

From equation (2.22), the field current is expressed as

$$i_{fd} = \frac{\Psi_{fd} - \Psi_{ad}}{L_{fd}} \tag{2.23}$$

The d-axis mutual flux linkage can be written as

$$\Psi_{ad} = -L_{ads} i_d + L_{ads} i_{fd}$$

$$= -L_{ads} i_d + \frac{L_{ads}}{L_{fd}} \left(\Psi_{fd} - \Psi_{ad}\right) \tag{2.24}$$

$$= L'_{ads} - i_d + \frac{\Psi_{fd}}{L_{fd}}$$

where

$$L_{aqs} = \left(\frac{1}{\frac{1}{L_{ads}} + \frac{1}{L_{fd}}}\right) \tag{2.25}$$

The mutual flux linkage of q-axis is given by

$$\Psi_{aq} = -L_{aqs} i_q \tag{2.26}$$

The air-gap torque is given by

$$T_e = \Psi_d i_q - \Psi_q i_d$$

$$= \Psi_{ad} i_q - \Psi_{aq} i_d \tag{2.27}$$

With pΨ terms and speed variations not considered (neglected), the stator voltage equations are

$$e_d = -R_a i_d - \Psi_q$$

$$= -R_a i_d + \left(L_l i_q - \Psi_{aq}\right) \quad (2.28)$$

$$e_q = -R_a i_q - \Psi_d$$

$$= -R_a i_q + (L_l i_d - \Psi_{ad}) \quad (2.29)$$

2.3.2 Network equations

There is only one machine, the machine network equations can be expressed in term of d-q reference frame. Referring to Fig 2.4 the machine terminal voltage and the infinite bus voltage in term of d-q components are

$$\tilde{E}_t = e_d + je_q \quad (2.30)$$

$$\tilde{E}_B = E_{Bd} + jE_{Bq} \quad (2.31)$$

From the system network equation

$$\tilde{E}_t = \tilde{E}_B + (R_E + jX_E)\tilde{I}_t$$

$$e_d + je_q = (E_{Bd} + jE_{Bq}) + (R_E + jX_E)\left(i_d + ji_q\right) \quad (2.32)$$

Again solving into d and q component gives

$$e_d = R_E i_d - X_E i_q + E_{Bd} \quad (2.33)$$

$$e_q = R_E i_q + X_E i_d + E_{Bq} \quad (2.34)$$

where

$$E_{Bd} = E_B sin\delta \quad (2.35)$$

$$E_{Bq} = E_B cos\delta \quad (2.36)$$

Manipulating the above equations, the expressions of i_d and i_q in terms of state variables are:

$$i_d = \frac{X_{Tq}[\Psi_{fd}\left(\frac{L_{ads}}{l_{ads}+L_{fd}}\right) - E_B cos\delta] - R_T E_B sin\delta}{D} \quad (2.37)$$

$$i_q = \frac{R_T\left[\Psi_{fd}\left(\frac{L_{ads}}{l_{ads}+L_{fd}}\right) - E_B cos\delta\right] + X_{Td}E_B sin\delta}{D} \tag{2.38}$$

where

$$R_T = R_a + R_E$$

$$X_{Tq} = X_E + \left(L_{aqs} + L_l\right) = X_E + X_{qs}$$

$$X_{Td} = X_E + (L'_{ads} + L_l) = X_E + X'_{ds} \tag{2.39}$$

$$D = R^2{}_T + X_{Tq}X_{Td}$$

where

X_{qs} , X'_{ds} = saturated values. (pu) = corresponding inductances.

2.3.3 Linearized system equations

Expressing equations (2.37) and (2.38) in terms of perturbed values, we get,

$$\Delta i_d = m_1\Delta\delta + m_2\Delta\Psi_{fd} \tag{2.40}$$

$$\Delta i_q = n_1\Delta\delta + n_2\Delta\Psi_{fd} \tag{2.41}$$

where

$$m_1 = \frac{E_{B(}X_{Tq}sin\delta_0 - R_T cos\delta_0)}{D}$$

$$n_1 = \frac{E_B(R_T sin\delta_{0+}X_{Td}cos\delta_0}{D}$$

$$m_2 = \frac{X_{Tq}}{D}\frac{L_{ads}}{\left(L_{ads} + L_{fd}\right)} \tag{2.42}$$

$$n_2 = \frac{R_T}{D}\frac{L_{ads}}{(L_{ads} + L_{fd})}$$

Now linearizing equations (2.24) and (2.26) and substituting the values from equations (2.40) and (2.41), we get

$$\Delta\Psi_{ad} = L'_{ads}(-\Delta i_d + \frac{\Delta\Psi_{fd}}{L_{fd}})$$

$$= \left(\frac{1}{L_{fd}} - m_2\right) L'_{ads}\Delta\Psi_{fd} - m_1 L'_{ads}\Delta\delta \qquad (2.43)$$

$$\Delta\Psi_{aq} = -L_{aqs}\Delta i_q$$

$$= -n_2 L_{aqs}\Delta\Psi_{fd} - n_1 L_{aqs}\Delta\delta \qquad (2.44)$$

Linearizing equation (2.23) and substituting the value from equation (2.43) gives

$$\Delta i_{fd} = \frac{\Delta\Psi_{fd} - \Delta\Psi_{ad}}{L_{fd}}$$

$$= \frac{1}{L_{fd}}\left(1 - \frac{L'_{ads}}{L_{fd}} + m_2 L'_{ads}\right)\Delta\Psi_{fd} + \frac{1}{L_{fd}} m_1 L'_{ads}\Delta\delta \qquad (2.45)$$

The linearized equation (2.24) is

$$\Delta T_e = \Psi_{ad0}\Delta i_q + i_{q0}\Delta\Psi_{ad} + \Psi_{aq0}\Delta i_d - i_{d0}\Delta\Psi_{aq}$$

Putting the values of Δi_d , Δi_q , $\Delta\Psi_{ad}$ and $\Delta\Psi_{aq}$ from equations (2.40) to (2.44), we obtain

$$\Delta T_e = K_1\Delta\delta + K_2\Delta\Psi_{fd} \qquad (2.46)$$

Where

$$K_1 = n_1\left(\Psi_{ad0} + L_{aqs} i_{d0}\right) - m_1\left(\Psi_{aq0} + L'_{ads} i_{q0}\right) \qquad (2.47)$$

$$K_2 = n_2\left(\Psi_{ad0} + L_{aqs} i_{d0}\right) - m_2\left(\Psi_{aq0} + L'_{ads} i_{q0}\right) + \frac{L'_{ads}}{L_{fd}} i_{q0} \qquad (2.48)$$

Linearizing equations (2.17) – (2.19) and substituting the values of Δi_{fd} and ΔT_e from equations (2.45) and (2.46), we get the system equations as

$$\begin{bmatrix} \Delta\dot{\omega}_r \\ \Delta\dot{\delta} \\ \Delta\dot{\Psi}_{fd} \end{bmatrix} = \begin{bmatrix} a_{11} & a_{12} & a_{13} \\ a_{21} & 0 & 0 \\ 0 & a_{32} & a_{34} \end{bmatrix} \begin{bmatrix} \Delta\omega_r \\ \Delta\delta \\ \Delta\Psi_{fd} \end{bmatrix} + \begin{bmatrix} b_{11} & 0 \\ 0 & 0 \\ 0 & b_{32} \end{bmatrix} \begin{bmatrix} \Delta T_m \\ \Delta E_{fd} \end{bmatrix} \qquad (2.49)$$

where

$$a_{11} = \frac{-K_D}{2H}$$

$$a_{12} = \frac{-K_1}{2H}$$

$$a_{13} = \frac{-K_2}{2H}$$

$$a_{21} = \omega_0 = 2\Pi f_0 \qquad (2.50)$$

$$a_{32} = -\frac{\omega_0 R_{fd}}{L_{fd}} m_1 L'_{ads}$$

$$a_{33} = -\frac{\omega_0 R_{fd}}{L_{fd}} (1 - \frac{L'_{ads}}{L_{fd}} + m_2 L'_{ads})$$

$$b_{11} = \frac{1}{2H}$$

$$b_{11} = \frac{\omega_0 R_{fd}}{L_{adu}}$$

ΔT_m and ΔE_{fd} depend on the prime-mover and the excitation controls. When constant mechanical input torque is, $\Delta T_m = 0$; and when constant exciter output voltage , ΔE_{fd} = 0.

In these equations mutual inductances are saturated values. The method of accounting for saturation for small signal analysis is defined below.

2.3.4 Representation of saturation in small-signal studies

Since we are expressing small-signal performance in terms of perturbed values of flux linkages and currents, a difference has to be made between incremental saturation and total saturation.

Total saturation is related with total values of flux linkages and currents. while the incremental saturation is related with perturbed values of flux linkages and currents. So ,the incremental slope of the saturation curve is used to computing the incremental saturation as shown in in the fig.

Representing the incremental saturation factor $K_{sd(incr)}$, we get

$$L_{ads(incr)} = K_{sd(incr)}L_{adu} \tag{2.51}$$

$$K_{sd(incr)} = \frac{1}{1 + B_{sat}A_{sat}e^{B_{sat}(\Psi_{at0}-\Psi_{T1})}} \tag{2.52}$$

Similar is the case for q-axis saturation.

Total saturation is used for computing the initial values of system variables. While incremental saturation is used for relating the perturbed values i.e. in equations (2.39) , (2.42) , (2.47) , (2.48) and (2.50), the incremental factor is used.

2.3.5 Summary of procedure for formulating the state matrix

step 1 The following parameters are given:

P_t Q_t E_t R_E X_E

L_d Lq L_l R_a L_{fd} R_{fd} A_{sat} B_{sat} Ψ_{T1}

step 2 The next is to compute the initial steady state values (denoted by subscript 0) of system variables:

I_t, power factor angle Φ

Total saturation factor K_{sd} and K_{sq}

$K_{sd} = K_{sq} = \frac{\Psi_{at}}{\Psi_{at}+\Psi_I}$; $\Psi_{at} = |\tilde{E}_a|$; $\Psi_I = A_{sat}e^{B_{sat}(\Psi_{at}-\Psi_{TI})}$; $\tilde{E}_a = \tilde{E}_t + (R_a + jX_l)\tilde{I}_t$

$$X_{ds} = L_{ds} = K_{sd}L_{adu} + L_l$$

$$X_{qs} = L_{qs} = K_{sq}L_{aqu} + L_l$$

$$\delta_i = tan^{-1}\left(\frac{I_tX_{qs}cos\Phi - I_tR_asin\Phi}{E_t + I_tR_acos\Phi + I_tX_{qs}sin\Phi}\right)$$

$$e_{d0} = E_t sin\delta_i$$

$$e_{q0} = E_t cos\delta_i$$

$$i_{d0} = I_t \sin(\delta_i + \Phi)$$

$$i_{q0} = I_t cos(\delta_i + \Phi)$$

$$E_{Bd0} = e_{d0} - R_E i_{d0} + X_E i_{q0}$$

$$E_{Bq0} = e_{q0} - R_E i_{q0} - X_E i_{d0}$$

$$\delta_0 = tan^{-1}(\frac{E_{Bd0}}{E_{Bq0}})$$

$$E_B = (E^2{}_{Bd0} + E^2{}_{Bq0})^{1/2}$$

$$i_{fd0} = \frac{e_{q0} + R_a i_{q0} + L_{ds} i_{d0}}{L_{ads}}, \quad E_{fd0} = L_{adu} i_{fd0}$$

$$\Psi_{ad0} = L_{ads}(-i_{d0} + i_{fd0}), \quad \Psi_{aq0} = -L_{aqs} i_{q0}$$

step 3 The next next step to compute incremental saturation factor and the corresponding saturated values of L_{ads} ,L_{aqs} ,L'_{ads} and then put in equations(2.39),(2.42),(2. 46) and (2.47)

step 4 Finally, we compute the matrix **A**.

Block diagram representation

Fig 2.5 shows the transfer function block diagram of the SMIB system.

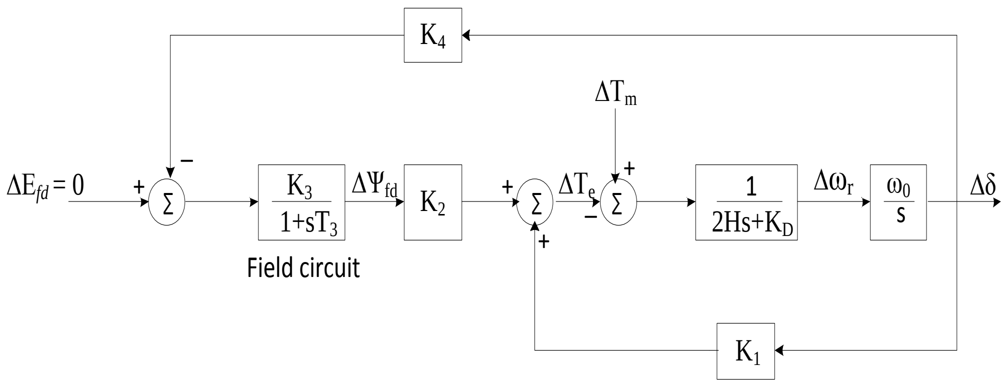

Fig 2.5 Transfer function block diagram representation of SMIB system with constant E_{fd}

2.4 EFFECTS OF THE EXCITATION SYSTEM

In this section, we will extend the state space model and develop the transfer function block diagram to include the excitation system. We will examine effect of the excitation system on the small signal stability performance of the SMIB system.

The excitation input control signal is normally the generator terminal voltage E_t..Here E_t is not a state variable . So, E_t has to be described in terms of the state variables.

E_t can be expressed in complex form as:

$$\tilde{\boldsymbol{E}}_{\boldsymbol{t}} = e_d + je_q$$

Hence,

$$E^2{}_t = e^2{}_d + e^2{}_q$$

Applying a small perturbation, we may write

$$(E_{t0} + \Delta E_t)^2 = (e_{d0} + \Delta e_d)^2 + (e_{q0} + \Delta e_q)^2$$

Now neglecting second-order terms involving perturbed values, we get

$$E_{t0}\Delta E_t = e_{d0}\Delta e_d + e_{q0}\Delta e_q$$

Therefore,

$$\Delta E_t = \frac{e_{d0}}{E_{t0}}\Delta e_d + \frac{e_{q0}}{E_{t0}}\Delta e_q \tag{2.53}$$

Equations (2.28) and (2.29) may be written (terms in perturbed values) as

$$\Delta e_d = -R_a\Delta i_d + L_l\Delta i_q - \Delta\Psi_{aq}$$

$$\Delta e_q = -R_a\Delta i_q - L_l\Delta i_d + \Delta\Psi_{ad}$$

Then we substitute the values of Δi_d , Δi_q , $\Delta\Psi_{ad}$ and $\Delta\Psi_{aq}$ in the above equations in terms of the state variables and get

$$\Delta E_t = K_5\Delta\delta + K_6\Delta\Psi_{fd} \tag{2.54}$$

where,

$$K_5 = \frac{e_{d0}}{E_{t0}}\left[-R_a m_1 + L_l n_1 + L_{aqs} n_1\right] + \frac{e_{q0}}{E_{t0}}\left[-R_a n_1 - L_l m_1 - L'_{ads} m_1\right] \tag{2.55}$$

$$K_6 = \frac{e_{d0}}{E_{t0}}\left[-R_a m_2 + L_l n_2 + L_{aqs} n_2\right] + \frac{e_{q0}}{E_{t0}}\left[-R_a n_2 - L_l m_2 - L'_{ads}\left(\frac{1}{L_{fd}} - m_2\right)\right] \tag{2.56}$$

For the purpose of examination and illustration of the effect on small signal stability, we will include the excitation system model as shown in Fig 2.6. We assume a thyristor excitation system.

A high exciter gain, without transient gain reduction or derivative feedback, is used. Component T_R represents the terminal voltage transducer time constant.

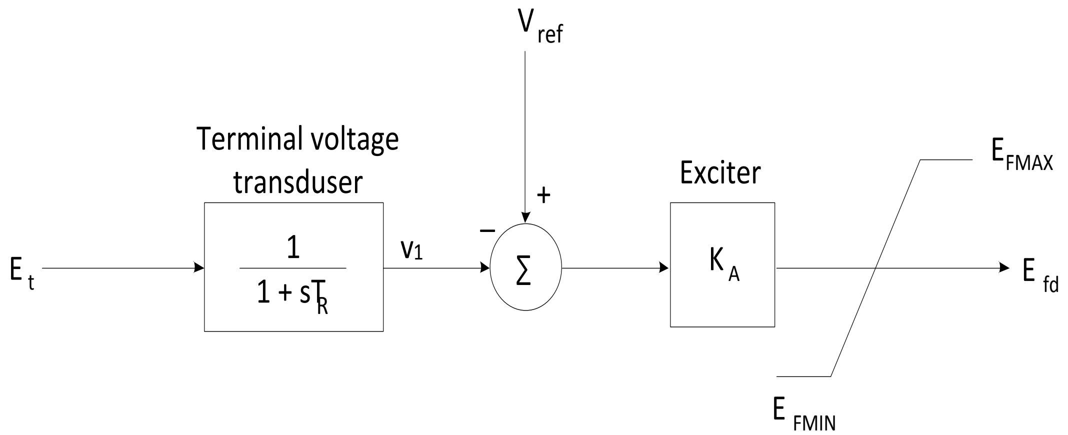

Fig 2.6 Block diagram of thyristor excitation system with AVR

The output voltage of the exciter is represented by E_{FMAX} and $E_{FMIN.}$ These limits are ignored for small disturbance studies as we are interested in a linearized model about an operating point such that E_{fd} within the limits.

From Fig 2.6, using perturbed values, we get

$$\Delta v_1 = \frac{1}{1 + pT_R} \Delta E_t$$

Hence,

$$p\Delta v_1 = \frac{1}{T_R} (\Delta E_t - \Delta v_1)$$

Substituting the value of ΔE_t in above equation from equation (54), we get

$$p\Delta v_1 = \frac{K_5}{T_R} \Delta\delta + \frac{K_6}{T_R} \Delta\Psi_{fd} - \frac{1}{T_R} \Delta v_1 \quad (2.56)$$

From Fig. 2.6

$$E_{fd} = K_A(V_{ref} - v_1)$$

In terms of perturbed value, we get

$$\Delta E_{fd} = K_A(-\Delta v_1) \quad (2.57)$$

The field circuit dynamic equation with the effect of the excitation system included, becomes

$$p\Delta\Psi_{fd} = a_{31}\Delta\omega_r + a_{32}\Delta\delta + a_{33}\Delta\Psi_{fd} + a_{34}\Delta v_1 \quad (2.58)$$

where

$$a_{34} = -b_{32}K_A = -\frac{\omega_0 R_{fd}}{L_{adu}} K_A \quad (2.59)$$

Since we have a first order model for the exciter, the new state variable added is Δv_1. from equation (2.56)

$$p\Delta v_1 = a_{41}\Delta\omega_r + a_{42}\Delta\delta + a_{43}\Delta\Psi_{fd} + a_{44}\Delta v_1 \quad (2.60)$$

Where

$$a_{41} = 0$$

$$a_{42} = \frac{K_5}{T_R}$$

$$a_{43} = \frac{K_6}{T_R} \qquad (2.61)$$

$$a_{44} = -\frac{1}{T_R}$$

Since $p\Delta\omega_r$ and $p\Delta\delta$ are not affected by the exciter,

$$a_{14} = a_{24} = 0$$

The complete state-space model for the power system including the excitation system has the following form:

$$\begin{bmatrix} \Delta\dot{\omega}_r \\ \Delta\dot{\delta} \\ \Delta\dot{\Psi}_{fd} \\ \Delta\dot{v}_1 \end{bmatrix} = \begin{bmatrix} a_{11} & a_{12} & a_{13} & 0 \\ a_{21} & 0 & 0 & 0 \\ 0 & a_{32} & a_{33} & a_{34} \\ 0 & a_{42} & a_{43} & a_{44} \end{bmatrix} \begin{bmatrix} \Delta\omega_r \\ \Delta\delta \\ \Delta\Psi_{fd} \\ \Delta v_1 \end{bmatrix} + \begin{bmatrix} b_1 \\ 0 \\ 0 \\ 0 \end{bmatrix} \Delta T_m \qquad (2.62)$$

With constant mechanical torque input,

$$\Delta T_m = 0$$

Block diagram representation including the excitation system

Fig 2.7 shows the transfer function block diagram obtained by including the voltage transducer and exciter blocks.

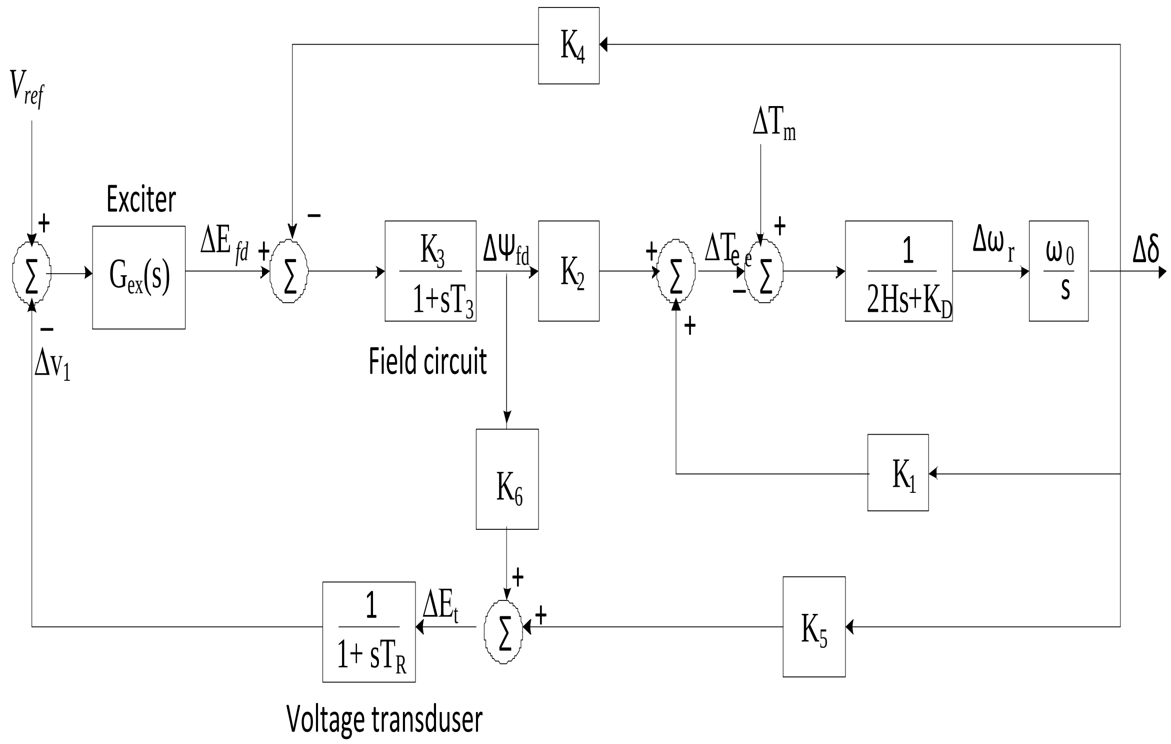

Fig 2.7 Transfer function block diagram representation including exciter and AVR

CHAPTER-3

STATIC VAR COMPENSATOR

3.1: INTRODUCTION

Static var compensator (SVCs) is a shunt-connected FACTS controller. It is a static generator and supplies/or absorbs reactive power to control specific parameters of the electric power system . The term "static" is used to indicate that's SVCs, unlike synchronous compensators, have no moving or rotating components.

Thus an SVC consists of static var generator (SVG) or absorber devices and a suitable control device.

SVCs are used to improve voltage and reactive power conditions in ac systems. An additional task of SVC is to increase transmission capacity as result of power oscillation damping.

The schematic diagram of a static var compensator is shown in Fig 3.1.

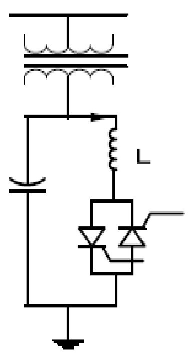

Fig 3.1   A static var compensator

3.1.1 Types of SVC:

The following are the basic types of elements which control reactive power in any static Var system.

- Saturated Reactor (SR)
- Thyristor Controlled Reactor (TCR)
- Thyristor - Swiched Capacitor (TSC)
- Thyristor Controlled Transformer (TCT)
- Self or Line Commutated Convertor (SCC / LCC)

3.2 STRUCTURE OF SVC CONTROLLERS

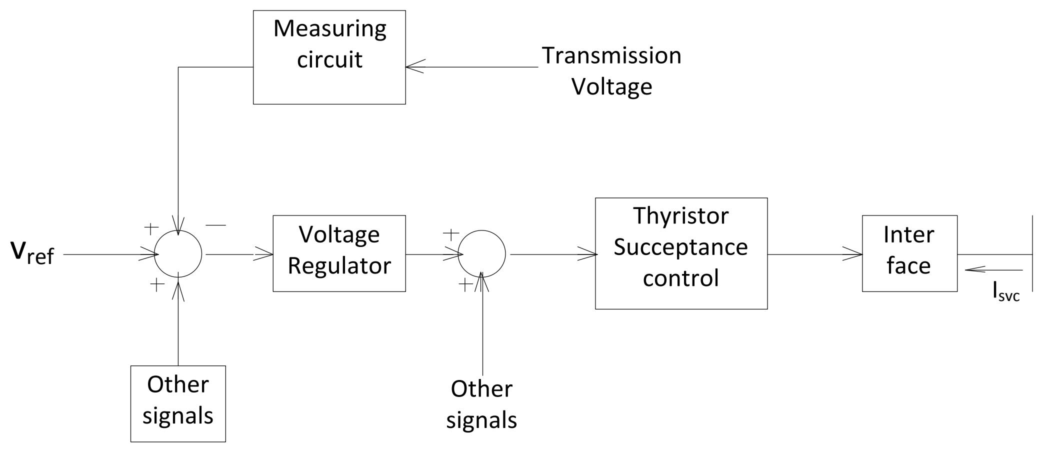

Fig 3.2: Block diagram representing of SVC control

Figure 3.2 shows the block diagram for voltage and damping control by a SVC. The voltage regulator is of the proportional type.

3.2.1 Effect of the SVC on synchronizing and damping torque

The influence of a SVC is integrated in the response of the i^{th} electromechanical mode as shown in the modified block diagram of Fig. 3.3 This diagram comprehensively demonstrates the individual effects of the SVC voltage regulator as well as the SVC auxiliary power swing damping controller (PSDC). The SVC can provide damping to the power system only if the auxiliary damping controllers are incorporated in the SVC control, which modulate the bus voltage in response to a control signal sensitive to power oscillations. Although both the synchronizing and damping-torque coefficients are influenced by the generator-excitation systems, only the damping torque is affected by the system loads and turbine governors.

SVC Voltage Regulator: This generates a susceptance reference signal, ΔB_{SVCi}, that primarily causes the bus voltage to change by ΔV_{Bi} through a function $K_{VBi}(s)$ representing the network response. The same susceptance output ΔB_{SVCi}, also generates a synchronizing-torque contribution by acting through a function $K_{TBi}(s)$. The SVC voltage regulator is represented by the transfer function $Vregi(s)$:

The modal voltage at the SVC bus is influenced by the modal speed δ_i and, consequently, by the modal angle ω_i both of which impart their contribution through the frequency-dependent function $K_{Vdi}(s)$,

SVC PSDC: An auxiliary control signal, $\Delta X_{\delta i}$, is provided as input to the SVC PSDC. As explained previously, this signal must be a function of the modal speed or modal angle $\Delta\delta_i$, to which its relationship must be expressed through the transfer function $Kxdi(s)$. The SVC PSDC is modeled by the transfer function $PSDCx(s)$ that contributes an additional modulating input ΔV_{modi} to the voltage regulator. The SVC susceptance ΔB_{SVCi}, generates an inner-loop response ΔX_{ILi} which influences the auxiliary signal through the transfer function $K_{xBi}(s)$.

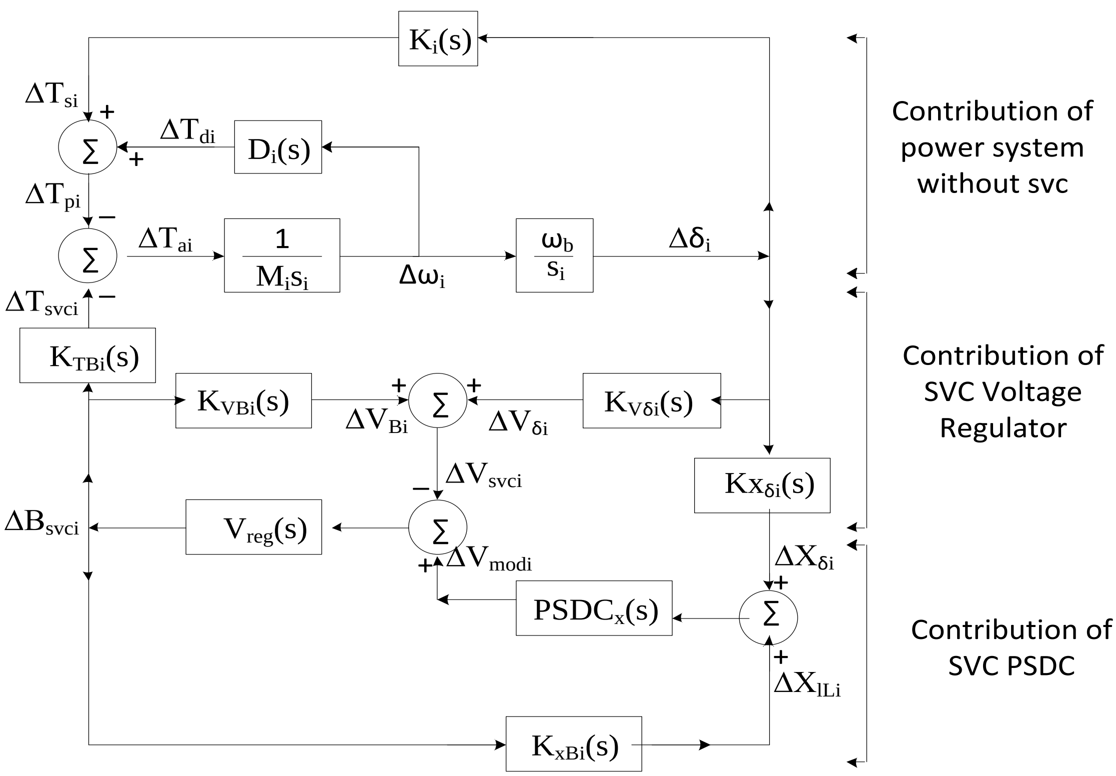

Figure 3.3 Transfer function block diagram representation showing model damping and synchronizing torque contributions

3.3 SVC VOLTAGE CONTROLLER

Fig 3.4 shows the voltage controller model. The gain K_R is reciprocal of the slope. The slope setting of K_R varies between 20 per unit (5% slope) and 100 per unit (1% slope) on the SVC base. The time constant, $T_{R,}$ is between 20 to 150 msec. The leg-lead terms are zero. The lag-lead terms can be used to provide adequate phase and margin. Integrators should be non – windup.

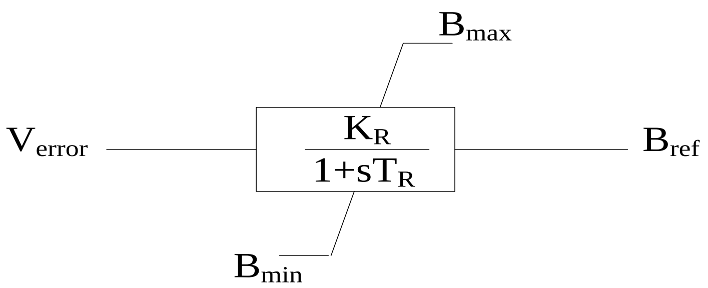

Figure 3.4 Block diagram of SVC voltage regulator model

3.4 SVC DAMPING CONTROLLER

Design Procedure for a PSDC

The following procedure is suggested in [11, 12] for the design of the auxiliary PSDC.

1. The controller is designed primarily for the dominant swing-mode frequency.

2. The desired phase angle of the controller-transfer function is obtained corresponding to the pure-damping condition. This phase angle is a function of the controllability and observability constants.

3. An operating point signifying a heavy-power transfer scenario is chosen and a specific magnitude of system damping is selected for this scenario. The desired controller gain is that which ensures the specific magnitude of damping for the chosen operating point subject to the following conditions:

a. an inner-loop gain margin of at least 10 dB is satisfied for the most constraining network configuration;

b. a maximum level of interaction with sub synchronous modes is ensured; and

c. a noise amplification beyond an acceptably small limit is not permitted.

4. The efficacy of the PSDC controller must be established for both forward and reverse power flow in the tie-line. A tentative value of controller gain can be obtained by performing stability simulations for the worst system configuration in the absence of PSDC and noting the maximum variation in the auxiliary signal magnitude. The gain maybe chosen as that which can cause the SVC reactive power to traverse its entire controllable range for this peak variation in the auxiliary control signal. A typical PSDC controller comprises a lead-lag stage, a washout stage, and a high-frequency–filtering stage, together with a gain [11] as shown in Fig. 3.5. The filter is designed to pass the swing-mode-frequency signal while allowing for any variation in this frequency from system conditions. It rejects frequencies associated with non–power-swing modes, such as sub synchronous torsional oscillations and modes relating to noise signals that override the auxiliary control signals. In some cases, this noise may be within the bandwidth of the power-swing frequencies. The control system, therefore, needs to be designed by avoiding too high a gain. This technique for PSDC controller design is valid for a two-area, three-area [11], [12] or a multi-area system. The effectiveness of the same SVC is dependent on the location of the loads as well as its own placement. The controllability of a mode may improve if the SVC is located close to the midpoint of that mode shape. In the event that the midpoints of different modes are at different locations, the damping benefit, which the SVC can provide for one mode, will not be the same as that for the other modes.

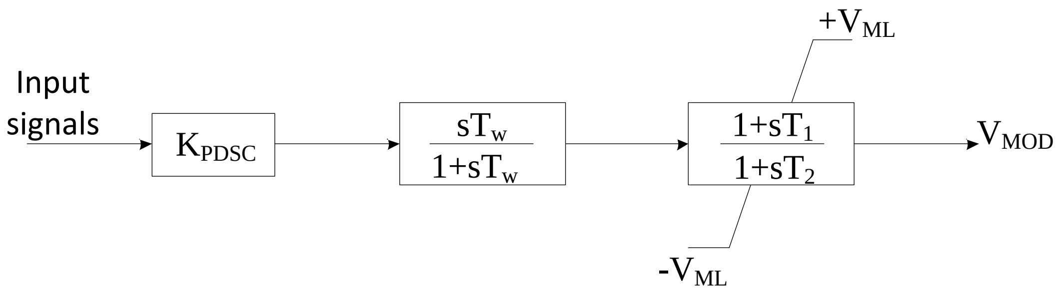

Figure 3.5 Block diagram of SVC damping controller model

CHAPTER-4

SYSTEM MODELLING

4.1 SYSTEM UNDER CONSIDERATION

The Single Machine Infinite Bus system is shown in fig 4.1. This system consists four 555 MVA, 24 kV, 60Hz thermal generating units. It is chosen to analyze the improvement of small signal stability by using SVC.

The system data and parameters are given in Appendix.

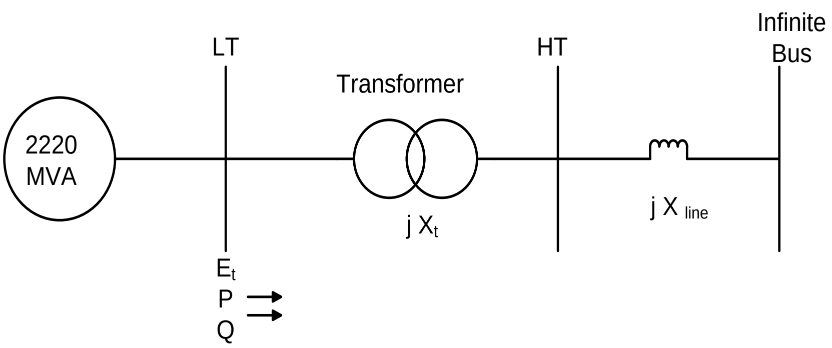

Fig. 4.1 Schematic diagram of SMIB system

4.2 ANALYSIS OF SMIB SYSTEM WITH SVC

The Static var compensator (SVC) is shunt-connected static generator or absorber whose output varies so as to control specific parameters of the electric power system. Thus a SVC consists of static var generator (SVG) or absorber devices and a suitable control device. It is used to improve voltage and reactive power conditions in ac systems. An additional task of SVC is to increase transmission capacity as result of power oscillation damping.

Fig. 4.2 shows the schematic diagram of SMIB system incorporating SVC at the midpoint of transmission line. The equivalent circuit diagram of SMIB system with SVC is shown in Fig. 4.3. It is shown that the SVC is represented by a susceptance B_{svc}. The generator is represented by an emf behind a transient reactance X_d'. All resistances in the system are neglected. When the SVC provide reactive power to the system it acts as a capacitor and vice-versa.

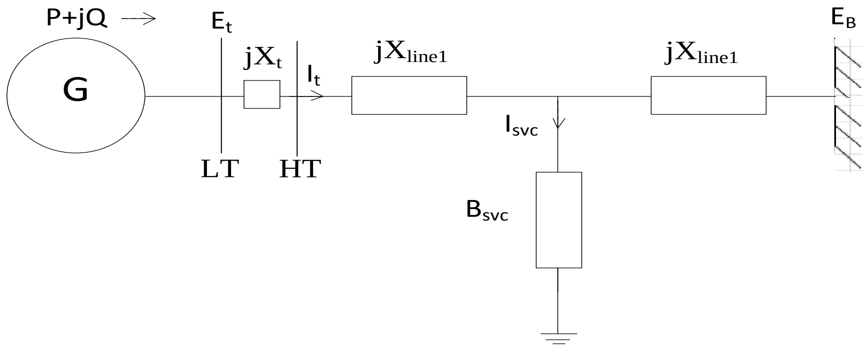

Fig 4.2 Schematic diagram of SMIB system installed with SVC at midpoint of line

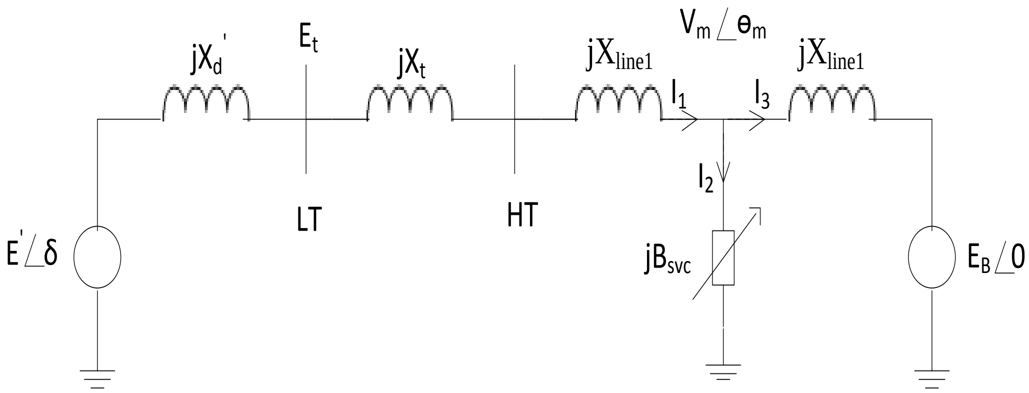

Fig 4.3 Equivalent circuit of system shown in Fig. 4.2

For the purpose of analysis, the circuit shown in Fig 4.3 can be reduced to the form of Fig 4.4 by using the Thevenin equivalent of the transmission network external to the machine and the adjacent transmission.

The small signal stability of the system of Fig 4.4 is analysed by accounting for the effects of the excitation system and the SVC voltage and damping controllers.

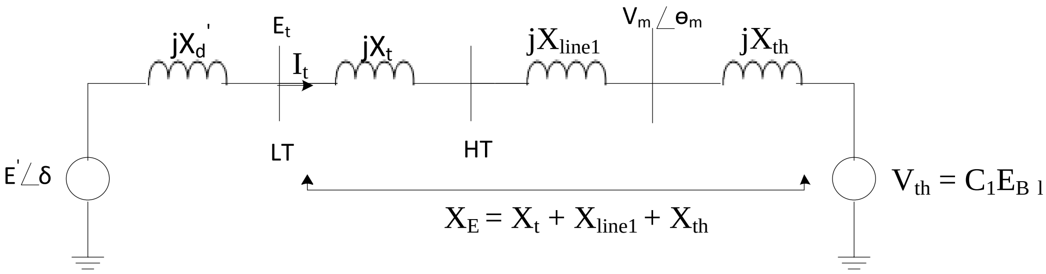

Fig 4.4 Thevenin equivalent circuit of SMIB power system installed with SVC

From Fig. 4.4

$$\boldsymbol{V_{th=}}C_1\boldsymbol{E_B}$$

$$Z_{th} = C_1 X_{line1}$$

where

$$C_1 = \frac{1}{1+\frac{X_{line1}}{X_{svc}}}$$

4.2.1 Effects of Synchronous Machine field Circuit Dynamics:

We now consider the system performance including the effect of field flux variations. The amortisseur effect will be neglected and the field voltage will be assumed constant (manual excitation control).

A state-space model of the system is developed by first reducing the synchronous machine equations to an appropriate form and then combining them with network equations. We will express time in seconds, angles in electrical radians, and all other variables in per unit.

4.2.1.1 Synchronous machine equations

As in the classical generator model, the acceleration equations are

$$p\Delta\omega_r = \frac{1}{2H}(T_m - T_e - K_D\Delta\omega_r) \quad (4.1)$$

$$p\delta = \omega_0\Delta\omega_r \quad (4.2)$$

where

$$\omega_0 = 2\Pi f_0 \text{ elec. rad/s.}$$

In this case, the q-axis leads the reference $\mathbf{E_B}$ by the angle δ. As shown in the Fig 4.5, the rotor angle δ is the sum of the angle δ_i (internal angle) and the angle by which **Et** leads $\mathbf{E_B}$. The choice of $\mathbf{E_B}$ as the reference for measuring rotor angle is convenient from the viewpoint of solution of network equations.

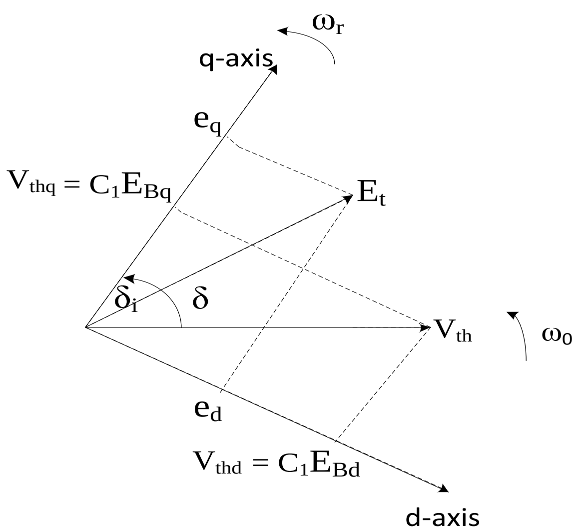

Fig 4.5 Relation between quantities in d-axis and q-axis

The field circuit dynamics equations are

$$p\Psi_{fd} = \omega_0(e_{fd}+R_{fd}i_{fd})$$

$$= \frac{\omega_0 R_{fd}}{L_{adu}} E_{fd} - \omega_0 R_{fd} i_{fd} \qquad (4.3)$$

$$\text{where} e_{fd} = \frac{R_{fd}}{L_{adu}} E_{fd}$$

where E_{fd} is the exciter output voltage. Equations (17) - (19) describe the dynamics of the synchronous machine with $\Delta\omega_r$, δ and Ψ_{fd} as the state variables.

With amortisseurs neglected, the equivalent circuits relating the machine flux linkages and current are as shown in Fig 4.6

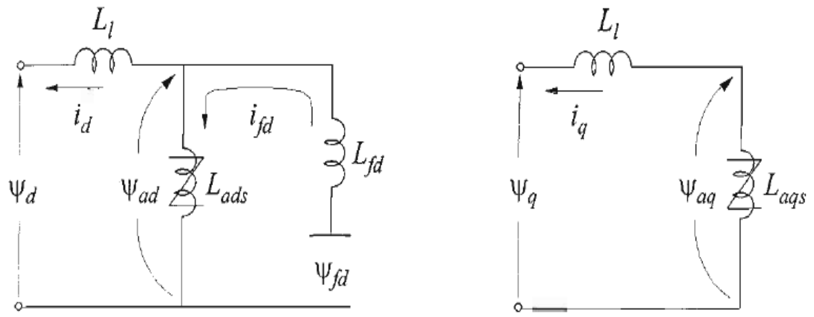

Fig 4.6 Equivalent circuit relating machine flux linkages and current

The rotor and stator flux linkages are given by

$$\Psi_d = -L_1 i_d + L_{ads}(-i_d + i_{fd})$$

$$= -L_1 i_d + \Psi_{ad} \quad (4.4)$$

$$\Psi_q = -L_1 i_q + L_{aqs}(-i_q)$$

$$= -L_1 i_q + \Psi_{aq} \quad (4.5)$$

$$\Psi_{fd} = L_{ads}(-i_d + i_{fd}) + L_{fd} i_{fd}$$

$$= \Psi_{ad} + L_{fd} i_{fd} \quad (4.6)$$

where

Ψ_{ad} , Ψ_{aq} =Air-gap (mutual) flux linkages

L_{aqs} = Saturated values of the mutual inductances

From equation (4.6), the field current is expressed as

$$i_{fd} = \frac{\Psi_{fd} - \Psi_{ad}}{L_{fd}} \quad (4.7)$$

The d-axis mutual flux linkage can be written as

$$\Psi_{ad} = -L_{ads} i_d + L_{ads} i_{fd}$$

$$= -L_{ads} i_d + \frac{L_{ads}}{L_{fd}}(\Psi_{fd} - \Psi_{ad}) \quad (4.8)$$

$$= L'_{ads}(-i_d + \frac{\Psi_{fd}}{L_{fd}})$$

where

$$L'_{ads} = (\frac{1}{\frac{1}{L_{ads}} + \frac{1}{L_{fd}}}) \quad (4.9)$$

The mutual flux linkage of q-axis is given by

$$\Psi_{aq} = -L_{aqs} i_q \quad (4.10)$$

By linearizing above equations, we get

$$\Delta\Psi_{ad} = L'_{ads}\left(-\Delta i_d + \frac{\Delta\Psi_{fd}}{L_{fd}}\right) \quad (4.11)$$

$$\Delta\Psi_{aq} = -L_{aqs}\Delta i_q \quad (4.12)$$

The air-gap torque is given by

$$T_e = \Psi_d i_q - \Psi_q i_d$$

$$= \Psi_{ad} i_q - \Psi_{aq} i_d \quad (4.13)$$

By linearizing the above equation, we get

$$\Delta T_e = \Psi_{ad0}\Delta i_q + i_{q0}\Delta\Psi_{ad} - \Psi_{aq0}\Delta i_d - i_{d0}\Delta\Psi_{aq} \quad (4.14)$$

With pΨ terms and speed variations not considered (neglected), the stator voltage equations are

$$e_d = -\Psi_q$$

$$= \left(L_l i_q - \Psi_{aq}\right) \quad (4.15)$$

$$e_q = -R_a i_q + \Psi_d$$

$$= -(L_l i_d - \Psi_{ad}) \tag{4.16}$$

4.2.1.2 Network Equations

The machine terminal and infinite bus voltage in terms of the d-axis and q-axis components are given below

$$\mathbf{E_t} = e_d + je_q \tag{4.17}$$

$$\mathbf{V_{th}} = \mathrm{C}_1\mathbf{E_B}$$

$$= C_1\{E_{BD} + jE_{Bq}\} \tag{4.18}$$

The network constraint equation is

$$\mathbf{E_t} = \mathbf{V_{th}} + \mathrm{j}\mathrm{X}_\mathrm{E}\mathbf{I_t}$$

$$(e_d + j_{ed}) = C_1\boldsymbol{E_B} + jX_E\boldsymbol{I_t}$$

$$= C_1\left(E_{Bd} + jE_{Bq}\right) + jX_E\left(I_{td} + I_{tq}\right) \tag{4.19}$$

Separating Into d-axis and q-axis Components are given by

$$e_d = -X_E I_q + C_1 E_{Bd} \tag{4.20}$$

$$e_q = X_E I_d + C_1 E_{Bq} \tag{4.21}$$

Where

$$E_{Bd} = E_{B\,sin\delta}$$

$$E_{Bq} = E_{B\,cos\delta}$$

By manipulating the above equations, the expressions of i_d and i_q in terms of the state variables are obtained as

$$i_d = \frac{L'_{ads}\frac{\Psi_{fd}}{L_{fd}} - C_1 E_B cos\delta}{L_l + X_E + L'_{ads}}$$

$$i_d = \frac{L'_{ads}\frac{\Psi_{fd}}{L_{fd}} - C_1 E_B cos\delta}{X_{Td}} \tag{4.22}$$

$$i_q = \frac{C_1 E_B sin\delta}{L_l + X_E + L_{aqs}}$$

$$i_q = \frac{C_1 E_B sin\delta}{X_{Tq}} \qquad (4.23)$$

where,

$$X_{Tq} = L_l + X_E + L_{aqs}$$

$$X_{Td} = L_l + X_E + L'_{ads} \qquad (4.24)$$

$$C_1 = \frac{1}{1 - B_{svc} X_{line1}}$$

$$X_E = X_t + X_{line1} + X_{th}$$

$$X_{th} = \frac{X_{line1}}{1 - B_{svc} X_{line1}}$$

4.2.1.3 Linearized system equations

Expressing equations (4.22) and (4.23) in terms of perturbed values, we get,

$$\Delta i_d = m_1 \Delta\delta + m_2 \Delta\Psi_{fd} + m_3 \Delta\alpha \qquad (4.25)$$

$$\Delta i_q = n_1 \Delta\delta + n_2 \Delta\Psi_{fd} + n_3 \Delta\alpha \qquad (4.26)$$

where

$$m_1 = \frac{E_B sin\delta}{\{(1 - B_{svc} X_{line1})(X_t + X_{line1} + L_l + L'_{ads}) + X_{line1}\}}$$

$$m_2 = \frac{\frac{L'_{ads}}{L_{fd}}(1 - B_{svc} X_{line1})}{\{(1 - B_{svc} X_{line1})(X_t + X_{line} + L_l + L'_{ads}) + X_{line1}\}}$$

$$m_3 = \frac{\{(1 - B_{svc} X_{line1})(X_t + X_{line1} + L_l + L'_{ads}) + X_{line1}\}\left\{\frac{L'_{ads}}{L_{fd}} X_{line1} \Psi_{fd}\right\}\left\{\frac{L'_{ads}}{L_{fd}}(1 - B_{svc} X_{line1})\Psi_{fd} - E_B cos\delta\right\} * \{(X_t + X_{line1} + L_l + L'_{ads})(X_{line1})\}}{(1 - B_{svc} X_{line1})(X_t + X_{line1} + L_l + L'_{ads}) + X_{line1}}$$

$$n_1 = \frac{E_B cos\delta}{\{(1 - B_{svc}X_{line1})(L_l + X_t + X_{line1} + L'_{ads}) + X_{line1}\}} \quad (4.27)$$

$$n_2 = 0$$

$$n_3 = \frac{(L_l + X_t + X_{line1} + L'_{ads})X_{line1}E_B sin\delta}{\{(1 - B_{svc}X_{line1})(L_l + X_t + X_{line1} + L'_{ads}) + X_{line1}\}}$$

The linearized equation of torque is obtained from equation (4.14) as

$$\Delta T_e = \Psi_{ad0}\Delta i_q + i_{q0}\Delta\Psi_{ad} - \Psi_{aq0}\Delta i_d - i_{d0}\Delta\Psi_{aq}$$

Substituting the values of Δi_d , Δi_q , $\Delta\Psi_{ad}$ and $\Delta\Psi_{aq}$ from equations (4.24), (4.25), (4.11) and (4.12), we obtain

$$\Delta T_e = K_{T\delta}\Delta\delta + K_{T\Psi fd}\Psi_{fd} + K_{T\alpha}\Delta\alpha \quad (4.28)$$

where

$$K_{T\delta} = -m_1\left(i_{q0}L'_{ads} + \Psi_{aq0}\right) + n_1(i_{d0}L_{aqs} + \Psi_{ad0})$$

$$K_{T\Psi fd} = -m_2\left(i_{q0}L'_{ads} + \Psi_{aq0}\right) + \frac{L'_{ads}}{L_{fd}} i_{q0} \quad (4.29)$$

$$K_{T\alpha} = -m_3\left(i_{q0}L'_{ads} + \Psi_{aq0}\right) + n_3(i_{d0}L_{aqs} + \Psi_{ad0})$$

Now putting the value of ΔT_e in equation (4.1), we get

$$p\Delta\omega_r = \frac{1}{2H}\{\Delta T_m - (K_{T\delta}\Delta\delta + K_{T\Psi fd}\Psi_{fd} + K_{T\alpha}\Delta\alpha)\}$$

$$p\Delta\omega_r = \frac{\Delta T_m}{2H} + a_{12}\Delta\delta + a_{13}\Delta\Psi_{fd} + K_{15}\Delta\alpha \quad (4.30)$$

where

$$a_{12} = -\frac{K_{T\delta}}{2H}$$

$$a_{13} = -\frac{K_{T\Psi fd}}{2H} \qquad (4.31)$$

$$a_{15} = \frac{K_{Tsvc}}{2H}$$

From equation (4.2)

$$p\Delta\delta = \omega_0 \Delta\omega_r$$

$$p\Delta\delta = a_{21}\Delta\omega_r \qquad (4.32)$$

Where

$$a_{21} = \omega_0 = 377$$

Linearizing equation (4.8), we get,

$$\Delta i_{fd} = \frac{\Delta\Psi_{fd} - \Delta\Psi_{ad}}{L_{fd}}$$

Putting value of Ψ_{ad} from equation (4.11), we get

$$\Delta i_{fd} = \frac{1}{L_{fd}}[\Delta\Psi_{fd} - L'_{ads}(-\Delta i_d + \frac{\Delta\Psi_{fd}}{L_{fd}})$$

Again, putting the value of Δi_d in above equation, we get

$$\Delta i_{fd} = \frac{1}{L_{fd}}\left[1 - \frac{L'_{ads}}{L_{fd}} + m_2 L'_{ads}\right)\Delta\Psi_{fd} + \frac{1}{L_{fd}} m_1 L'_{ads}\Delta\delta$$

$$+\frac{L'_{ads}}{L_{fd}} m_3 \Delta\alpha \qquad (4.33)$$

Linearizing equation (4.3), we get

$$p\Delta\Psi_{fd} = \frac{\omega_0 R_{fd}}{L_{adu}}\Delta E_{fd} - \omega_0 R_{fd}\Delta i_{fd} \qquad (4.34)$$

Now putting the value of Δi_{fd} in above equation from equation (4.30),we get

$$p\Delta\Psi_{fd} = \frac{\omega_0 R_{fd}}{L_{adu}}\Delta E_{fd} - \omega_0 R_{fd}\frac{1}{L_{fd}}\left[(1 - \frac{L'_{ads}}{L_{fd}} + m_2 L'_{ads}\right)\Delta\Psi_{fd} + \frac{1}{L_{fd}} m_1 L'_{ads}\Delta\delta$$

$$+\frac{L'_{ads}}{L_{fd}} m_3 \Delta\alpha] \qquad (4.35)$$

4.2.2 Effects of excitation system

In this section, we will extend the state space model by including the effect of the excitation system.

The excitation input control signal is normally the generator terminal voltage $E_{t..}$ Here E_t is not a state variable . So, E_t has to be described in terms of the state variables.

E_t can be expressed in complex form:

$$\widetilde{\boldsymbol{E}}_{\boldsymbol{t}} = e_d + je_q$$

Hence,

$$E^2{}_t = e^2{}_d + e^2{}_q$$

Applying a small perturbation, we may write

$$(E_{t0} + \Delta E_t)^2 = (e_{d0} + \Delta e_d)^2 + (e_{q0} + \Delta e_q)^2$$

Now neglecting second-order terms involving perturbed values, we get

$$E_{t0}\Delta E_t = e_{d0}\Delta e_d + e_{q0}\Delta e_q$$

Therefore,

$$\Delta E_t = \frac{e_{d0}}{E_{t0}}\Delta e_d + \frac{e_{q0}}{E_{t0}}\Delta e_q \qquad (4.36)$$

From equations (4.15) and (4.16) may be written (terms in perturbed values) as

$$\Delta e_d = L_l \Delta i_q - \Delta\Psi_{aq} \qquad (4.37)$$

$$\Delta e_q = -L_l \Delta i_d + \Delta\Psi_{ad} \qquad (4.38)$$

Now putting the values of Δi_d , Δi_q, $\Delta\Psi_{ad}$ and $\Delta\Psi_{aq}$ from previous equations in the above equations in terms of the state variables and putting the resulting expressions for Δe_d and Δe_q in equation (4.36), we get

$$\Delta E_t = K_{E\delta}\Delta\delta + K_{E\Psi fd}\Psi_{fd} + K_{E\alpha}\Delta\alpha \tag{4.39}$$

Where

$$K_{E\delta} = \frac{e_{d0}}{E_{t0}}\left(L_l + L_{aqs}\right)n_1 - \frac{e_{q0}}{E_{t0}}\left(L_l + L'_{ads}\right)m_1$$

$$K_{E\Psi fd} = \frac{e_{q0}}{E_{t0}}\left[-L_l m_2 + L'_{ads}\left(\frac{1}{L_{fd}} - m_2\right)\right] \tag{4.40}$$

$$K_{E\alpha} = \frac{e_{d0}}{E_{t0}}\left(L_l + L_{aqs}\right)n_3 - \frac{e_{q0}}{E_{t0}}\left(L_l + L'_{ads}\right)m_3$$

We now include the excitation system model shown in fig 2.6. It represents a thyristor excitation system. A high exciter gain, without transient gain reduction or derivative feedback, is used. Component T_R represents the terminal voltage transducer time constant.

The output voltage of the exciter is represented by E_{FMAX} and $E_{FMIN.}$ These limits are ignored for small disturbance studies, we are interested in a linearized model about an operating point such that E_{fd} is within the limits.

From Fig. 2.6, using perturbed values, we get

$$\Delta v_1 = \frac{1}{1 + pT_R}\Delta E_t$$

Hence,

$$p\Delta v_1 = \frac{1}{T_R}\left(\Delta E_t - \Delta v_1\right)$$

Substituting the value of ΔE_t in above equation from equation (4.36), we get

$$p\Delta v_1 = \frac{1}{T_R}\left(K_{E\delta}\Delta\delta + K_{E\Psi fd}\Psi_{fd} + K_{E\alpha}\Delta\alpha - \Delta v_1\right) \qquad (4.41)$$

From the block diagram of thyristor excitation system with AVR

$$E_{fd} = K_A(V_{ref} - v_1)$$

In terms of perturbed value, we get

$$\Delta E_{fd} = K_A(-\Delta v_1) \qquad (4.42)$$

The field circuit dynamic equation with the effect of excitation system included, becomes

$$p\Delta\Psi_{fd} = a_{32}\Delta\delta + a_{33}\Delta\Psi_{fd} + a_{34}\Delta v_1 + a_{35}\Delta\alpha \qquad (4.43)$$

Where

$$a_{32} = -\frac{\omega_0 R_{fd}}{L_{fd}} m_1 L'_{ads}$$

$$a_{33} = -\frac{\omega_0 R_{fd}}{L_{fd}}\left(1 - \frac{L'_{ads}}{L_{fd}} + m_2 L'_{ads}\right) \qquad (4.44)$$

$$a_{34} = -K_A \frac{\omega_0 R_{fd}}{L_{adu}}$$

$$a_{35} = -\frac{\omega_0 R_{fd}}{L_{fd}} m_1 L'_{ads}$$

Since we have a first order model for the exciter, the new state variable added is Δv_1. from equation (4.41), we get

$$p\Delta v_1 = a_{42}\Delta\delta + a_{43}\Delta\Psi_{fd} + a_{44}\Delta v_1 + a_{45}\Delta\alpha \qquad (4.45)$$

Where

$$a_{42} = \frac{K_{E\delta}}{T_R}$$

$$a_{43} = \frac{K_{E\Psi fd}}{T_R}$$

$$a_{44} = -\frac{1}{T_R} \qquad (4.46)$$

$$a_{45} = \frac{K_{E\alpha}}{T_R}$$

4.2.3 Auxiliary input signal*:*

From Fig. 4.4, the auxiliary control signal $\left|\tilde{I}_{line}\right|$ can be expressed as follows.

$$\tilde{\mathbf{I}}_{\mathbf{line}} = \tilde{\mathbf{I}}_{\mathbf{t}}$$

Therefore $\tilde{\mathbf{I}}_{\mathbf{line}}$ can be expressed in complex form:

$$\tilde{\mathbf{I}}_{\mathbf{line}} = i_d + ji_q$$

Hence,

$$I^2{}_{line} = i^2{}_d + i^2{}_q$$

Applying a small perturbation, we may write

$$(I_{line0} + \Delta I_{line})^2 = (i_{d0} + \Delta i_d)^2 + (i_{q0} + \Delta i_q)^2$$

By neglecting second-order terms involving perturbed values, we get

$$I_{line0}\Delta I_{line} = i_{d0}\Delta i_d + i_{q0}\Delta i_q$$

Therefore,

$$\Delta I_{line} = \frac{i_{d0}}{I_{line0}}\Delta i_d + \frac{i_{q0}}{I_{line0}}\Delta i_q \qquad (4.47)$$

Now substituting the values of Δi_d and Δi_q in above equation, We get

$$\Delta I_{line} = K_{I\delta}\Delta\delta + K_{I\Psi fd}\Psi_{fd} + K_{I\alpha}\Delta\alpha \qquad (4.48)$$

Where

$$K_{I\delta} = \frac{i_{d0}}{I_{line0}}m_1 + \frac{i_{q0}}{I_{line0}}n_1$$

$$K_{I\Psi fd} = \frac{i_{d0}}{I_{line0}}m_2 \qquad (4.49)$$

$$K_{I\alpha} = \frac{i_{d0}}{I_{line0}}m_3 + \frac{i_{q0}}{I_{line0}}n_3$$

4.2.4 Voltage at the mid-point of the transmission line (v_m):

Let δ be the angle by which **E'** leads the infinite bus voltage $\mathbf{E_B}$.. From figure 4.3, applying KCL,

$$\bar{I}_1 = \bar{I}_2 + \bar{I}_3$$

$$\frac{\bar{\mathbf{E}}_t - \bar{\mathbf{V}}_m}{j(X_t + X_{line})} = jB_{svc}\bar{\mathbf{V}}_m + \frac{\bar{\mathbf{V}}_m - \mathbf{E_B}}{jX_{line1}}$$

$$D_{11}\bar{\mathbf{V}}_m = X_{11}\mathbf{E_B} + X_{line1}\bar{\mathbf{E}}_t$$

Where

$$X_{11} = X_t + X_{line1}$$

$$D_{11} = X_{line1} - B_{svc}X_{line1}X_{11} + X_{11}$$

$\mathbf{V_m}$ can be expressed in terms of d-axis and q-axis quantities as

$$(V_{md} + jV_{mq}) = \frac{X_{11}}{D_{11}}(E_{Bd} + jE_{Bq}) + \frac{X_{line1}}{D_{11}}(e_d + je_q)$$

Equating real and imaginary parts

$$V_{md} = \frac{X_{11}}{D_{11}}E_{Bd} + \frac{X_{line1}}{D_{11}}e_d \qquad (4.50)$$

$$V_{mq} = \frac{X_{11}}{D_{11}}E_{Bq} + \frac{X_{line1}}{D_{11}}e_q \qquad (4.51)$$

Hence,

$$V^2{}_m = V^2{}_{md} + V^2{}_{mq}$$

Applying a small perturbation, we may write

$$(V_{m0} + \Delta V_m)^2 = (V_{md0} + \Delta V_{md})^2 + (V_{mq0} + \Delta V_{mq})^2$$

By neglecting second-order terms involving perturbed values, we get

$$V_{m0}\Delta V_m = V_{md0}\Delta V_{md} + V_{mq0}\Delta V_{mq}$$

$$\Delta V_m = K_{m1}\Delta E_{Bd} + K_{m2}\Delta E_{Bq} + K_{m3}\Delta e_d + K_{m4}\Delta e_q + K_{m5}\Delta D_{11} \tag{4.52}$$

Where

$$K_{m1} = \frac{X_{11}}{V_{m0}{D^2}_{11}}(X_{11}E_{Bd0} + X_{line1}e_{d0})$$

$$K_{m2} = \frac{X_{11}}{V_{m0}{D^2}_{11}}(X_{11}E_{Bq0} + X_{line1}e_{q0})$$

$$K_{m3} = \frac{X_{line1}}{V_{m0}{D^2}_{11}}(X_{line1}e_{d0} + X_{11}E_{Bd0})$$

$$K_{m4} = \frac{X_{line1}}{V_{m0}{D^2}_{11}}(X_{line1}e_{q0} + X_{line1}E_{Bq0})$$

$$K_{m5} = -\frac{D_{110}}{V_{m0}{D^4}_{11}}[{X^2}_{11}{E^2}_{Bd0} + {X^2}_{line1}{e^2}_{d0} + 2X_{11}X_{line1}E_{Bd0}e_{d0} +$$

$${X^2}_{11}{E^2}_{Bq0} + {X^2}_{line1}{e^2}_{q0} + 2X_{11}X_{line1}E_{Bq0}e_{q0}]$$

The linearized equations of e_d, e_q, E_{Bd}, E_{Bq}, and D_{11} are given below:

$$\Delta e_d = L_l\Delta i_q - \Delta\Psi_{aq}$$

$$\Delta e_q = -L_l\Delta i_d + \Delta\Psi_{ad}$$

$$\Delta E_{Bd} = E_B cos\delta_0\Delta\delta$$

$$\Delta E_{Bq} = -E_B sin\delta_0\Delta\delta$$

$$\Delta D_{11} = -X_{11}X_{line1}C_2\Delta\alpha$$

Now putting the values of Δi_d, Δi_q, $\Delta\Psi_{ad}$ and $\Delta\Psi_{aq}$ from previous equations to above equations in terms of the state variables and then putting the resulting expressions for Δe_d, Δe_q, ΔE_{Bd}, ΔE_{Bq}, *and* ΔD_{11} in equation (4.45), we get

$$\Delta V_m = K_{v\delta}\Delta\delta + K_{v\Psi fd}\Psi_{fd} + K_{v\alpha}\Delta\alpha \tag{4.53}$$

Where

$$K_{v\delta} = K_{m1}E_B cos\delta_0 - K_{m2}E_B sin\delta_0 + K_{m3}n_1(L_l + L_{aqs}) - K_{m4}m_1(L_l + L'_{ads})$$

$$K_{v\Psi fd} = K_{m4}\left\{-m_2L_l + L'_{ads}\left(\frac{1}{L_{fd}} - m_2\right)\right\} \qquad (4.54)$$

$$K_{v\alpha} = K_{m3}n_3(L_l + L_{aqs}) - K_{m4}m_3(L_l + L'_{ads}) - K_{m5}X_{11}X_{line1}$$

4.3 INCORPORATION OF SVC VOLTAGE AND DAMPING CONTROLLER

SVC voltage controller along with a damping controller using line current auxiliary signal is shown in Fig 4.7.

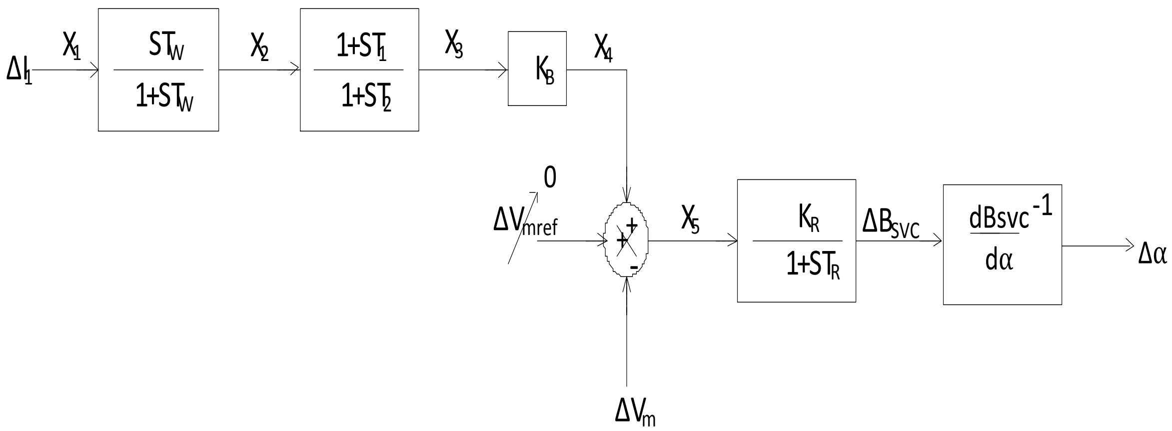

Fig. 4.7 Block diagram of SVC voltage controller along with a damping controller

From the block diagram

$$x_1 = \Delta I_{line} = K_{I\delta}\Delta\delta + K_{I\Psi fd}\Psi_{fd} + K_{I\alpha}\Delta\alpha$$

$$x_2 = K_B x_1$$

$$x_3 = \frac{sT_w}{1 + sT_w}x_2$$

$$x_4 = \frac{1 + sT_1}{1 + sT_2} x_3 \tag{4.55}$$

$$x_5 = x_4 - \Delta Vm$$

By using SVC voltage and damping controller the equations are linearized as

$$\Delta\alpha = (\frac{K_R}{1 + sT_R}) x_5 (\frac{1}{\frac{dB_{svc}}{d\alpha}})$$

$$p\Delta\alpha = a_{52}\Delta\delta + a_{53}\Delta\Psi_{fd} + a_{55}\Delta\alpha + a_{57}x_4 \tag{4.56}$$

where

$$a_{52} = -\frac{K_R}{T_R} K_{v\delta}$$

$$a_{53} = -\frac{K_R}{T_R} K_{v\Psi fd}$$

$$a_{55} = -\left(\frac{1}{T_R} + \frac{K_R}{T_R}\right) K_{v\alpha} \tag{4.57}$$

$$a_{57} = \frac{K_R}{T_R}$$

From equation (4.55)

$$x_3 = \frac{sT_w}{1 + sT_w} x_2$$

$$px_3 = a_{61}\Delta\omega_r + a_{62}\Delta\delta + a_{63}\Delta\Psi_{fd} + a_{64}\Delta v_1 + a_{65}\Delta\alpha + a_{66}x_3$$

$$+ a_{67}x_4 \tag{4.58}$$

Where

$$a_{61} = K_B K_{I\delta} a_{21}$$

$$a_{62} = K_B \{K_{I\Psi fd} a_{32} + K_{I\alpha} a_{52}\}$$

$$a_{63} = K_B\{K_{I\Psi fd}a_{33} + K_{I\alpha}a_{53}\}$$

$$a_{64} = K_B K_{I\Psi fd}a_{34}$$

$$a_{65} = K_B\{K_{I\Psi fd}a_{35} + K_{I\alpha}a_{55}\}$$

$$a_{66} = -\frac{1}{T_w} \tag{4.59}$$

$$a_{67} = K_B K_{I\alpha}a_{57}$$

From equation (4.55)

$$\mathrm{x}_4 = \frac{1 + \mathrm{sT}_1}{1 + \mathrm{sT}_2}\mathrm{x}_3$$

$$px_4 = a_{71}\Delta\omega_r + a_{72}\Delta\delta + a_{73}\Delta\Psi_{fd} + a_{74}\Delta v_1 + a_{75}\Delta\alpha + a_{76}x_3 + a_{77}x_4 \tag{4.60}$$

Where

$$a_{71} = \frac{T_1}{T_2}a_{61}$$

$$a_{72} = \frac{T_1}{T_2}a_{62}$$

$$a_{73} = \frac{T_1}{T_2}a_{63}$$

$$a_{74} = \frac{T_1}{T_2}a_{64}$$

$$a_{75} = \frac{T_1}{T_2}a_{65}$$

$$a_{76} = \frac{1}{T_2} + \frac{T_1}{T_2}a_{66} \tag{4.61}$$

$$a_{77} = -\frac{1}{T_2} + \frac{T_1}{T_2}a_{67}$$

The complete state-space model, including the voltage and damping controller has the following form-

$$\begin{bmatrix} \Delta\dot{\omega}_r \\ \Delta\dot{\delta} \\ \Delta\dot{\Psi}_{fd} \\ \Delta\dot{v}_1 \\ \Delta\dot{\alpha} \\ \dot{x}_2 \\ \dot{x}_3 \end{bmatrix} = \begin{bmatrix} 0 & a_{12} & a_{13} & 0 & a_{15} & 0 & 0 \\ a_{21} & 0 & 0 & 0 & 0 & 0 & 0 \\ 0 & a_{32} & a_{33} & a_{34} & a_{35} & 0 & 0 \\ 0 & a_{42} & a_{43} & a_{44} & a_{45} & 0 & 0 \\ 0 & a_{11} & a_{11} & 0 & a_{11} & 0 & a_{11} \\ a_{61} & a_{62} & a_{63} & a_{64} & a_{65} & a_{66} & a_{67} \\ a_{71} & a_{72} & a_{73} & a_{74} & a_{75} & a_{76} & a_{77} \end{bmatrix} \begin{bmatrix} \Delta\omega_r \\ \Delta\delta \\ \Delta\Psi_{fd} \\ \Delta v_1 \\ \Delta\alpha \\ x_2 \\ x_3 \end{bmatrix} + \begin{bmatrix} \frac{1}{2H} \\ 0 \\ 0 \\ 0 \\ 0 \\ 0 \\ 0 \end{bmatrix} \Delta T_m \qquad (4.62)$$

4.4 REPRESENTATION OF SATURATION IN SMALL-SIGNAL STUDIES

Since we are analysing the small-signal performance in terms of the perturbed values of flux linkages and currents, a difference has to be made between incremental saturation and total saturation.

Total saturation is related with total values of flux linkages and currents. while the incremental saturation is related with perturbed values of flux linkages and currents. So, the incremental slope of the saturation curve is used for computing the incremental saturation.

Representing the incremental saturation factor $K_{sd(incr)}$, we get

$$L_{ads(incr)} = K_{sd(incr)} L_{adu} \qquad (4.63)$$

$$K_{sd(incr)} = \frac{1}{1 + B_{sat} A_{sat} e^{B_{sat}(\Psi_{at0} - \Psi_{T1})}} \qquad (4.64)$$

In a similar manner, the factor for q-axis saturation can be determined.

Total saturation is used for computing the initial values of system variable. While incremental saturation is used for relating the perturbed values i.e. in equations (4.24), (4.27), (4.29), (4.31) and (4.46), the incremental factor is used.

4.5 SUMMARY OF PROCEDURE FOR FORMULATING THE STATE MATRIX

step 1 The following parameters are given:

P_t Q_t E_t R_E X_E

L_d Lq L_l R_a L_{fd} R_{fd} A_{sat} B_{sat} Ψ_{T1}

step 2 The next is to compute the initial steady state values (denoted by subscript 0) of system variables:

I_t, power factor angle Φ

Total saturation factor K_{sd} and K_{sq}

$$K_{sd} = K_{sq} = \frac{\Psi_{at}}{\Psi_{at}+\Psi_I} \ ; \Psi_{at} = |\tilde{E}_a| \ ; \Psi_I = A_{sat}e^{B_{sat}(\Psi_{at}-\Psi_{TI})} \ ;$$

$$\tilde{E}_a = \tilde{E}_t + (R_a + jX_l)\tilde{I}_t$$

$$X_{ds} = L_{ds} = K_{sd}L_{adu} + L_l$$

$$X_{qs} = L_{qs} = K_{sq}L_{aqu} + L_l$$

$$\delta_i = tan^{-1}(\frac{I_tX_{qs}cos\Phi - I_tR_asin\Phi}{E_t+I_tR_acos\Phi + I_tX_{qs}sin\Phi})$$

$$e_{d0} = E_tsin\delta_i$$

$$e_{q0} = E_tcos\delta_i$$

$$i_{d0} = I_t\sin(\delta_i + \Phi)$$

$$i_{q0} = I_tcos(\delta_i + \Phi)$$

$$v_{md0} = e_{d0} + x_{11}i_{q0}$$

$v_{mq0} = e_{q0} - x_{11} i_{d0}$

$i_{2d0} = -B_{svc} v_{mq0}$

$i_{2q0} = B_{svc} v_{md0}$

$i_{3d0} = i_{d0} - i_{2d0}$

$i_{3q0} = i_{q0} - i_{2q0}$

$E_{Bd0} = v_{md0} + x_{line1} i_{3q0}$

$E_{Bq0} = v_{mq0} - x_{line1} i_{3q0}$

$\delta_0 = tan^{-1}(\frac{E_{Bd0}}{E_{Bq0}})$

$E_B = (E^2{}_{Bd0} + E^2{}_{Bq0})^{1/2}$

$i_{fd0} = \frac{e_{q0} + R_a i_{q0} + L_{ds} i_{d0}}{L_{ads}}$, $E_{fd0} = L_{adu} i_{fd0}$

$\Psi_{ad0} = L_{ads}(-i_{d0} + i_{fd0})$, $\Psi_{aq0} = -L_{aqs} i_{q0}$

step3 the next next step to compute incremental saturation factor and the corresponding saturated values of L_{ads} ,L_{aqs} ,L'_{ads} and then put in equations (4.39), (4.42), (4.46) and (4.47).

step4 Finally, we compute the matrix **A**.

CHAPTER 5

CASE STUDIES AND RESULTS

5.1 SMIB SYSTEM WITHOUT ANY SVC

At first, the system is analysed without any SVC. The system data and operating conditions are given in Appendix. The SVC controller parameters are given below:

$$B_{svc} = 0\,, K_b = 0\,, K_R = 0$$

5.1.1 Rotor angle deviation : The plots of rotor angle deviations with time for 5% change in mechanical torque corresponding to transmitted active powers of P=0.5 p.u. and 1.0 p.u. are shown in Fig. 5.1 and 5.2, respectively.

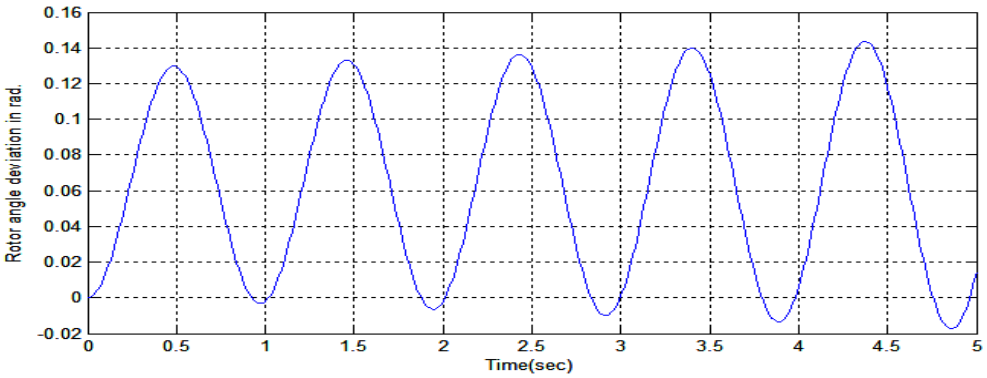

Fig 5.1 Plot of rotor angle deviation vs. time without SVC for P=0.5 p.u.

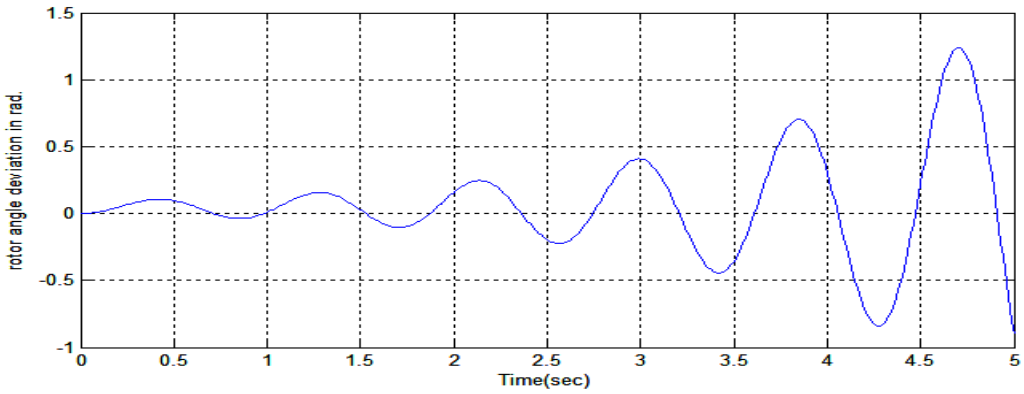

Fig 5.2 Plot of rotor angle deviation vs. time without SVC for P=1.0 p.u.

From Fig. 5.1 and 5.2, it can be observed that the small signal stability of the system decreases as the transmitted active power is increased from 0.5 p.u to 1 p.u.

5.1.2 Damping ratio: The transmitted active power was gradually varied from P=0.2 p.u to 1.0 p.u. The eigenvalues of the state matrices were computed. Fig 5.3 shows the plot of the damping ratio of the rotor mode eigenvalues against the transmitted active power. It is again observed that the system becomes small signal unstable for higher values of active power transmitted.

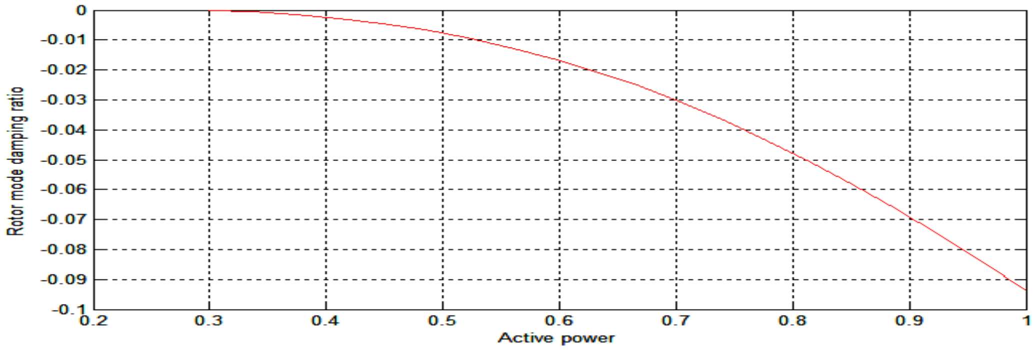

Fig 5.3 Plot of rotor mode damping ratio with ‘P’ (without SVC)

5.2 SMIB SYSTEM WITH SVC VOLTAGE CONTROLLER ONLY

The system was analysed with SVC voltage controller only. The SVC firing angle is set to 160^0. The controller parameters are given below:

$$K_R = 20\,, T_R = 0.02\; s, \qquad T_1 = 1s,\; T_2 = 0.1s, T_w = 1s$$

5.2.1 Rotor angle deviation: In this case, the transmitted active power is P =1.0 p.u. The plot of rotor angle deviation with time for 5% change in mechanical torque is shown in Fig 5.4.

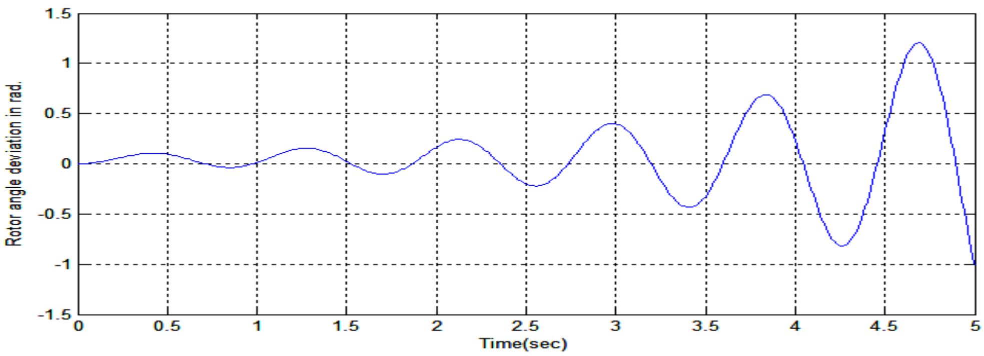

Fig 5.4 Rotor angle deviation vs. time with SVC voltage controller only (P=1.0 p.u)

5.2.2 Damping ratio: The line active power was gradually varied from P=0.2 to 1.0 p.u..The SVC firing angle is kept unchanged at 160^0. Fig 5.5 shows the plot of the damping ratio of the rotor mode eigenvalues against the line active power. It is observed that as compared to the case without any SVC, the system small signal stability is marginally improved with only the SVC voltage controller.

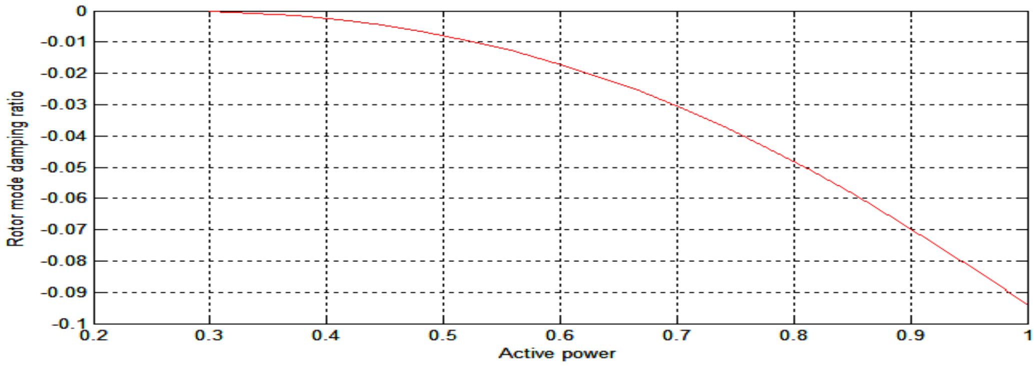

Fig 5.5 Plot of rotor mode damping ratio vs. ‘P’ (with SVC voltage controller only)

5.3 SMIB SYSTEM WITH BOTH SVC VOLTAGE AND DAMPING CONTROLLERS:

The system was analysed with the SVC voltage controller along with a damping controller. The parameters for the damping controller are given below:

$$K_b = 0.05\,, K_R = 20\,, T_R = 0.02\ s, \qquad T_1 = 1s, T_2 = 0.1s, T_w = 1s$$

5.3.1 Rotor angle deviation: The transmitted active power is P =1.0 p.u. The SVC firing angle is kept at 160^0. The plot of rotor angle deviation with time for 5% change in mechanical torque is shown in Fig. 5.6. It can be observed that the system small signal stability is markedly improved.

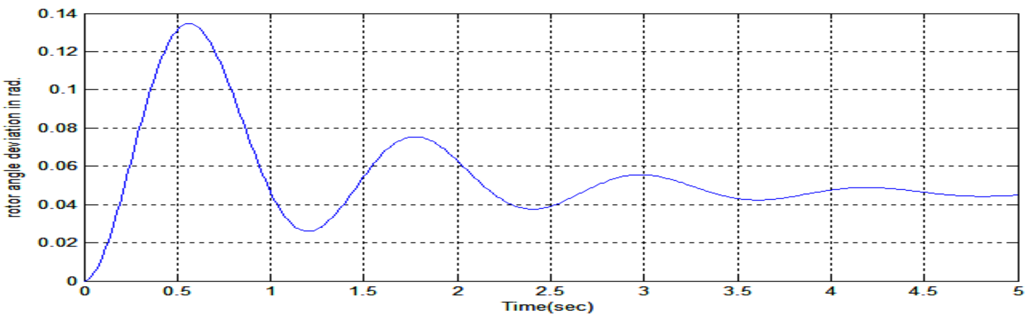

Fig 5.6: Plot of rotor angle deviation vs. time (with SVC voltage and damping controller)

5.3.2 Damping ratio: The SVC firing angle is kept at 160^0. The transmitted active power was varied from P=0.2 to 1.0p.u. The eigenvalues of the state matrix were computed. The damping ratio of the rotor mode eigenvalues are plotted against the transmitted active power. Fig 5.7 shows the plot of the damping ratio of the rotor mode eigenvalues against the transmitted active power. It is observed that the system small signal stability is markedly improved.

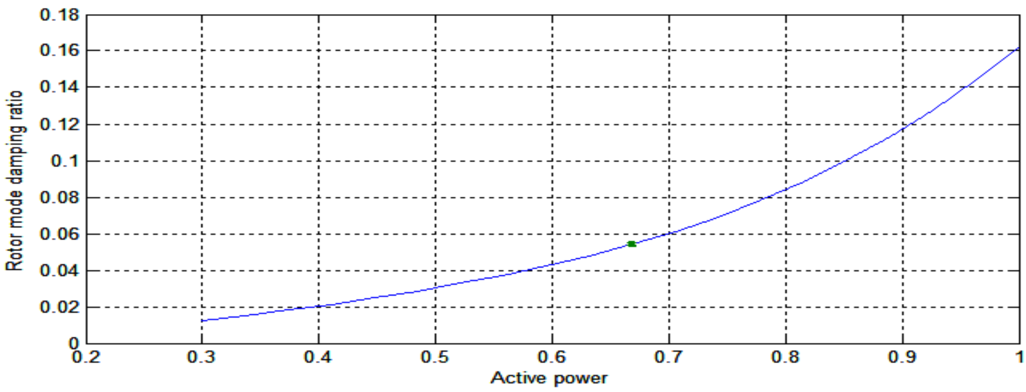

Fig 5.7 Plot of rotor mode damping ratio vs. 'P' (with SVC voltage and damping controller)

5.4 COMPARISON:

5.1.1 Rotor angle deviation: The SVC firing angle is kept at 160^0. The line active power is set to P=1.0p.u. The eigenvalues of the state matrix were computed. Fig. 5.8 shows the comparison of rotor angle deviation vs. time without SVC and with SVC controllers for 5% change in mechanical torque. It can be observed that with the SVC voltage controller, there is very little improvement in system damping. On the other hand, with both the SVC voltage and damping controllers, the system damping is markedly improved.

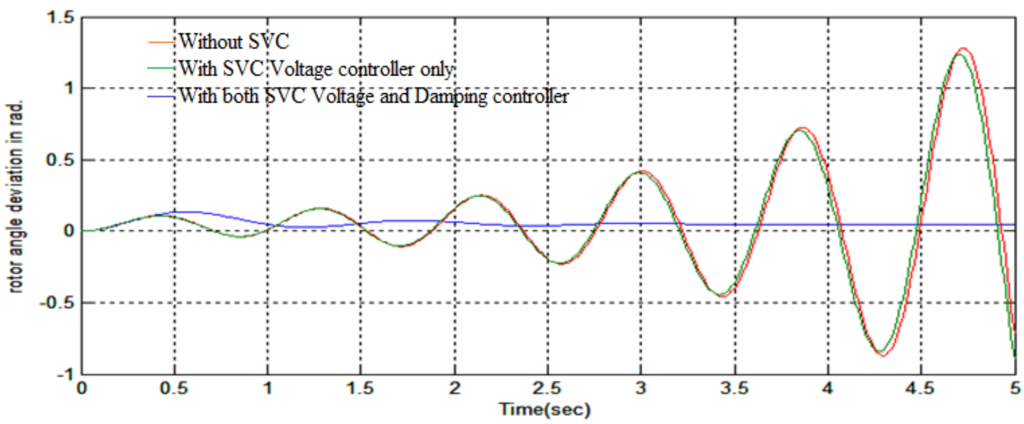

Fig. 5.8 shows the comparison of Rotor angle deviation without SVC and with SVC controllers (P = 1.0 p.u.)

5.1.2 Damping ratio: SVC firing angle is kept at 160^0. The transmitted active power was varied from P=0.2 to 1.0 p.u. The eigenvalues of the state matrix were computed. Fig 5.9 shows the plots of the damping ratio of the rotor mode eigenvalues against the transmitted active power corresponding to three cases namely, without any SVC, with SVC voltage controller only and with both the SVC voltage and damping controllers. It is observed that the system small signal stability only marginally improves with the SVC voltage controller while marked improvement is observed with both the SVC voltage and damping controllers.

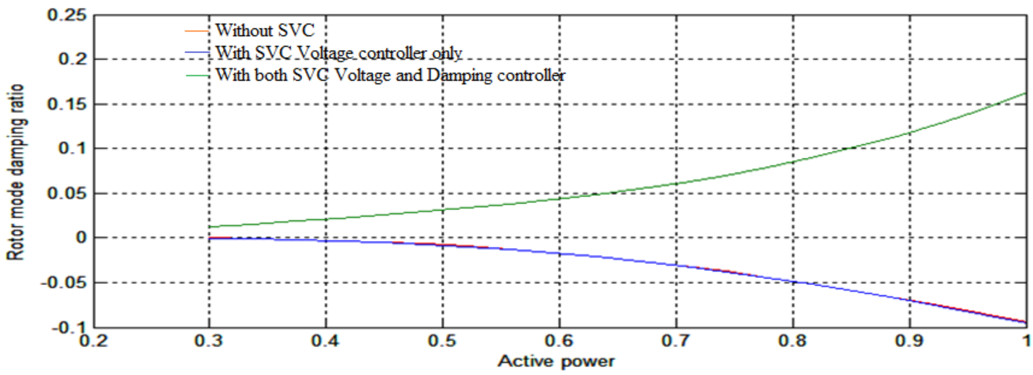

Fig 5.9:Plots of the damping ratio vs. 'P' without SVC, with SVC voltage controller only and with both the SVC voltage and damping controllers

CONCLUSIONS

In this work, the small signal stability of a single machine infinite bus system is analysed. A SVC is connected at the mid point of the long transmission line. The SVC comprises a voltage controller in conjunction with a damping controller. It is observed that SVC with only voltage controller is only marginally able to improve the small signal stability of the system. However, when a damping controller is added to the voltage controller, the small signal stability of the system shows a marked improvement. The line current magnitude is taken as an auxiliary signal for the SVC damping controller.

SCOPE FOR FURTHER WORK

- In this work, the line current signal is used as the supplementary control signal. Other supplementary signals like synthesized frequency deviation, active power deviation etc may be used for studying the small signal stability of the system.
- Initial value of SVC firing angle / susceptance may be varied to see the effect on the small signal stability.
- The SVC damping controller parameters have to be properly tuned for an optimum response. The parameters are dependent on the system operating condition. An adaptive controller may be designed to account for the same.

APPENDIX

The operating conditions of SMIB system are:

$$P = 0.9 p.u. \quad Q = 0.3\, p.u, \quad E_t = 1.0 p.u.$$

The transformer and line reactance are considered 0.15 and 0.5 p.u on the base of 2220 MVA, 24 kV respectively.

All the generators are represented by an equivalent generator model including the effect of the generator field circuit dynamics. The parameters of each of the four generators of the plant in per unit on its rating are as follows:

$$X'_d = 0.3 p.u. \; H = \frac{3.5 MWs}{MVA} w_0 = 377 \frac{rad}{s}$$

$$X_d = 1.81 \; X_q = 1.76$$

$$X_l = 0.16 \; L_{adu} = 1.65 \; L_{aqs} = 1.60 \; L_l = 0.16$$

$$R_{fd} = 0.0006 \, L_{fd} = 0.153.$$

$$A_{sat} = 0.031 \quad B_{sat} = 6.93 \quad \Psi_{T1} = 0.8$$

PUBLICATIONS

[1] R. Meena, S. Khan, S. Bhowmick, "Power Oscillation Damping of a Single Machine Infinite Bus System Using SVC Line Current Auxiliary Signal" ETEEE National Conference, Vol. 1 pp. 46-52, Feb. 2015. (Published)

[2] R. Meena, S. Khan, S. Bhowmick, "Small Signal Stability Improvement of a Single Machine Infinite Bus System Using SVC " INDICON IEEE International Conference 2015. (Communicated)

REFERENCES

[1] IEEE Task Force, "Proposed term and definitions for power system stability,"IEETrans.,Vol. PAS-101, pp. 1894-1898, July 1982.

[2] P. Kundur, *“Power System Stability and Control”,* Tata McGraw Hill, 2006.

[3] A.M. Lyapunov, Stability of motion, English translation, Academic Press, Inc.,1967.

[4] G.C. Verghese, I.J. Perez-Arriaga, and F.C. Schweppe, "Selective Model Analysis with Application to Electric Power System, Part I: Heuristic Introduction, Part II: The Dynamic Stability Problem," IEEE Trans., Vol., PAS-101, NO. 9, pp. 3117-3134, September 1982.

[5] R.T. Byerly, R.J. Bennon, and D.E. Sherman, "Eigenvalue Analysis of Synchronizing Power Flow Oscillation in Large Electric Power Systems,"IEEE Trans., Vol., PAS-101. 235-243, January 1982.

[6] W.G. Heffron and R.A. Phillips, "Effects of Modern Amplidyne Voltage Regulator in Underexcited Operation of Large Turbine Generators," AIEE Trans., Vol. PAS-71, pp. 692-697, August 1952.

[7] F.P. deMello and C. Corcordia, "Concepts of Synchronous Machine Stability as Affected by Eexcitation Control," IEEE Trans Vol. PAS-88, pp. 316-329, April 1969.

[8] CIGRE Task Force 38-01-02, Static %r Compensutors,1986.

[9] Suman Bhowmick “A Comparison of Commonly used Input Signals for Power Oscillation Damping” IEEE INDICON, 2004 pp 456-459.

[10] Carson W. Taylor, IEEE Special Stability Controls Working Group. "SVC models for Power Flow and Dynamic Performance ," IEEE Trans., Vol.9,No. 1, February 1994.

[11] E.V. Larsen and J.H. Chow, "SVC Control Design for System Dynamic Performance," IEEE Special Symposium on Application of SVS for System Dynamic Performance, Publication 87TH0187-5-PWR, 1987., pp. 36–53

[12] The Electric Power Research Institute (EPRI) Report TR-100696, “Improved Static VAR Compensator Control,” Final Report of Project 2707-01, Prepared by General Electric (GE) Company, Schenectady, NY, June 1992.

[13] E.V. Larsen and Joe Chow, “Concepts for Design of FACTS Controllers to Damp Power Swings,” in IEEE Trans. Power Systems, Vol.lO, No.2. May 1995, pp. 948-955.

[14] H.F.Wang and F.J.Swift, “A Unified Model for The Analysis of FACTS Devices in Damping Power System Oscillations - Part-I,’’ IEEE Trans Power Deliv.;Vo1.12, No.2, April 1997. pp. 941-946.

[15] E.Z Zhou, “Application of Static Var Compensators to increase power system damping”, IEEE Transactions onPower Systems, Vol. 8, No. 2, May1993, pp 655-661.

[16] E. Lerch, D. Povh and L.Xu“Advanced Control for Damping Power System Oscillations”, IEEE Trans. on Power Systems, Vol. 6, No. 2, May 1991 pp 524-535.

[17] H.F Wang and F.J Swift, “Capability of the Static Var Compensator in Damping Power System Oscillations” IEE Proc. Genr. Transm. Distrib.,Vol 143, No. 4, July 1996, pp 353-358.

[18] E.V. ben and Joe Chow,. “Application of Static Var Systems for System Dynamic Performance,” IEEE Publicntion no. S7TH0187-SPWR.

[19] E. Lareen, N. Miller, S. Nilsson, and S. Lindgren,“Benefits of GTO-Based Compensation Systems for Electric Utility Applications,” IEEE/PES paper 91 SM 397-0 PWRD

[20] G. Sybille, L. Gerin-Lajoie, and P. Giroux, “Interactions Between Static Var Compensators and Series Compensation on Hydro-Quebec 735 kV Network,” *CEA Transactions of Engineering and Operating Division*, Paper 92-SP-181, Vol. 31, Pt. 4, 1992.

[21] L. Gerin-Lajoie, G. Scott, S. Breault, E. V. Larsen, D. H. Baker, and A. F. Imece, “Hydro-Quebec Multiple SVC Application Control Stability Study,” *IEEE Transactions on Power Delivery*, Vol. 5, No. 3, July 1990, pp. 1543–1551.

[22] K. R. Padiyar and R. K. Varma, “Damping Torque Analysis of Static Var System Controllers,” *IEEE Transactions on Power Systems*, Vol. 6, No. 2, May 1991, pp. 458–465.

[23] K. R. Padiyar and R. K. Varma, “Concepts of Static Var System Control for Enhancing Power Transfer in Long Transmission Lines,” *Electric Machines and Power Systems*, Vol. 18, No. 4–5, July–October 1990, pp. 337–358.

[24] E. V. Larsen, D. H. Baker, A. F. Imece, L. Gerin-Lajoie, and G. Scott, “Basic Aspects of Applying SVCs to Series-Compensated ac Transmission Lines,” *IEEE Transactions on Power Delivery*, Vol. 5, No. 3, July 1990, pp. 1466–1473.

[25] L. Gerin-Lajoie, G. Scott, S. Breault, E. V. Larsen, D. H. Baker, and A. F. Imece, “Hydro-Quebec Multiple SVC Application Control Stability Study,” *IEEE Transactions on Power Delivery*, Vol. 5, No. 3, July 1990, pp. 1543–1551.

[26] A. E. Hammad, “Applications of Static Var Compensators in Utility Power Systems,” IEEE Special Publication 87TH0187-5-PWR, *Application of Static Var Systems for System Dynamic Performance*, 1987, pp. 2–35.

[27] M. Parniani and M. R. Iravani, “Optimal Robust Control Design of Static Var Compensator,” *IEEE Transactions on Power Delivery*.

[28] Q. Zhao and J. Jiang, “Robust SVC Controller Design for Improving Power System Damping,” *IEEE Transactions on Power Systems*, Vol. 10, No. 4, November 1995.

[29] A. E. Hammad and M. El-Sadek, “Application of a Thyristor-Controlled Var Compensator for Damping Sub synchronous Oscillations in Power Systems,” *IEEE Transactions on Power Apparatus and Systems*, Vol. 103, No. 1, January 1984, pp. 198–211.

[30] Y. Y. Hsu and C. J. Wu, “Design of PID Static Var Controller for the Damping of subsynchronous Oscillations,” *IEEE Transactions on Energy Conversion*, Vol. 3, No. 2, June 1988, pp. 210–216.

[31] K. R. Padiyar and R. K. Varma, “Static Var System Auxiliary Controller for Damping Torsional Oscillations,” *International Journal of Electrical Power and Energy Systems*, Vol. 12, No. 4, October 1990, pp. 271–286.

[32] A. E. Hammad, “Analysis of Power System Stability Enhancement by Static Var Compensators,” IEEE Transactions on Power Systems, Vol. PTllrRS-1, No. 4, pp.222-227, November 1986.